https://doi.org/10.5194/bg-2021-280
Preprint. Discussion started: 29 October 2021

Biogeosciences Discussions
Open Access
EGU

Controls on nitrite oxidation in the upper Southern Ocean: insights from winter kinetics experiments in the Indian sector

Mhlangabezi Mdutyana[1,2*], Tanya Marshall[1], Xin Sun[3,4], Jessica M. Burger[1], Sandy J. Thomalla[2,5], Bess B. Ward[3] and Sarah E. Fawcett[1,5]

[1]Department of Oceanography, University of Cape Town, Rondebosch, South Africa
[2]Southern Ocean Carbon and Climate Observatory (SOCCO), CSIR, Rosebank, South Africa
[3]Department of Geosciences, Princeton University, Princeton, New Jersey, USA
[4]Department of Ecology and Evolutionary Biology, Yale University, New Haven, Connecticut, USA
[5]Marine and Antarctic Research centre for Innovation and Sustainability (MARIS), University of Cape Town, Cape Town, South Africa
[*]Corresponding author: M. Mdutyana, mdtmhl001@myuct.ac.za

Abstract

Across the Southern Ocean in winter, nitrification is the dominant mixed-layer nitrogen cycle process, with some of the nitrate produced therefrom persisting to fuel productivity during the subsequent growing season, potentially weakening the spring/summer biological CO_2 sink. To better understand the controls on Southern Ocean nitrification, we conducted nitrite oxidation kinetics experiments in surface waters across the western Indian sector in winter. While all experiments (seven in total) yielded a Michaelis-Menten relationship with substrate concentration, the nitrite oxidation rates only increased substantially once the nitrite concentration exceeded 115±2.3 to 245±18 nM, suggesting that nitrite oxidizing bacteria (NOB) require a minimum (i.e., "threshold") nitrite concentration to produce nitrate. The half-saturation constant ranged from 134±8 to 403±24 nM, indicating a relatively high affinity of Southern Ocean NOB for nitrite, in contrast to results from culture experiments. Despite the high affinity of NOB for nitrite, its concentration rarely declines below 150 nM in the Southern Ocean's mixed layer, regardless of season. In the upper mixed layer, we measured ammonium oxidation rates that were two- to seven-fold higher than the coincident rates of nitrite oxidation, indicating that nitrite oxidation is the rate-limiting step for nitrification in the winter Southern Ocean. The decoupling of ammonium and nitrite oxidation, combined with a possible nitrite concentration threshold for NOB, may explain the non-zero nitrite that persists throughout the Southern Ocean's mixed layer year-round. We hypothesize that the apparent threshold nitrite requirement of NOB indicates nitrite undersaturation of the heme-rich nitrite oxidoreductase enzyme, perhaps driven by the limited availability of iron in surface waters.

https://doi.org/10.5194/bg-2021-280
Preprint. Discussion started: 29 October 2021

1. Introduction

The cycling of nitrogen (N) in the upper ocean is central to the role that phytoplankton and bacteria play in atmospheric carbon dioxide (CO_2) consumption and production. Annually, the Southern Ocean accounts for ~35% of total oceanic CO_2 removal (DeVries et al., 2017; Gruber et al., 2019; Watson et al., 2020) and absorbs ~40% of anthropogenic CO_2 (Khatiwala et al., 2009; Hauck et al., 2015; Gruber et al., 2019; Watson et al., 2020). The contribution of biology to CO_2 drawdown can be evaluated using the new production paradigm, among other approaches. This framework defines phytoplankton growth on nitrate (NO_3^-) supplied from below the euphotic zone as "new production" and phytoplankton growth on ammonium (NH_4^+) recycled within the euphotic zone as "regenerated production" (Dugdale and Goering 1967). Over appropriate timescales, new production is equivalent to "export production", the latter referring to the organic matter produced by phytoplankton that escapes recycling in surface waters and sinks into the ocean interior, thereby sequestering atmospheric CO_2 at depth (Dugdale and Goering, 1967; Eppley and Peterson ,1979; Volk and Hoffert, 1985; Raven and Falkowski, 1999). The occurrence of nitrification in the euphotic zone, which produces regenerated NO_3^-, complicates applications of the new production paradigm since phytoplankton growth fuelled by this NO_3^- will drive no net removal of CO_2(Yool et al., 2007).

In the Southern Ocean, nitrification appears to be largely confined to the dark waters below the euphotic zone during the summertime period of maximum NO_3^- consumption by phytoplankton (DiFiore et al., 2009; Mdutyana et al., 2020). By contrast, the Southern Ocean winter is characterized by elevated mixed-layer nitrification, coincident with low rates of NO_3^- uptake (Smart et al., 2015; Mdutyana et al., 2020). Some of the NO_3^- regenerated in the winter mixed layer will be supplied to phytoplankton during the proceeding spring and summer growing season, with negative implications for CO_2 removal on an annual basis. That said, there is evidence that ammonia oxidizing archaea, the organisms that are dominantly responsible for NH_4^+ oxidation (the first step in the nitrification pathway) (Beman et al., 2008; Newell et al., 2011; Peng et al., 2016) have a high iron requirement (Shafiee et al., 2019), such that NH_4^+ oxidation may at times experience iron limitation (Mdutyana, 2021). If this limitation is verified and proves widespread in the environment, one implication is that the iron-deplete conditions of the surface Southern Ocean may restrict mixed-layer nitrification and by extension, its putative role in weakening the biological CO_2 sink.

Nitrification is a chemoautotrophic process involving two pathways usually facilitated by different groups of microorganisms. The first step is NH_4^+ oxidation, which involves the oxidation of NH_4^+ via hydroxylamine and nitric oxide to NO_2^- (Walker et al., 2010; Vajrala et al., 2013; Kozlowski et al., 2016; Caranto and Lancaster, 2017) by ammonia oxidizing archaea and bacteria (AOA and AOB, respectively; collectively, ammonia oxidizing organisms, AOO). The second step is the oxidation of

https://doi.org/10.5194/bg-2021-280
Preprint. Discussion started: 29 October 2021

NO_2^- to NO_3^- by nitrite oxidizing bacteria (NOB), a polyphyletic group of microbes that is not well-understood in the ocean (Watson et al., 1986; Beman et al., 2013; Daims et al., 2016; Pachiadaki et al., 2017; Sun et al., 2021). In general, NO_2^- oxidation rate data are limited, with few rate measurements available for the Southern Ocean (Bianchi et al., 1997; Mdutyana et al., 2020; Olson, 1981a). Such measurements are critical, however, if we are to better understand the controls on nitrification in the Southern Ocean mixed layer and the connection between NO_3^- production by NOB and its subsequent removal by phytoplankton.

One approach for investigating the controls on NO_2^- oxidation is through experiments designed to yield a hyperbolic Michaelis-Menten relationship between NO_2^- oxidation rate and NO_2^- concentration. Useful kinetic parameters can be derived from this relationship, such as the maximum oxidation rate (V_{max}) and the half-saturation constant (K_m), with the latter indicating the NO_2^- concentration at which the oxidation rate equals $V_{max}/2$. Estimates of K_m provide information regarding the efficiency of NOB in acquiring substrate NO_2^-, with a lower K_m indicating a higher affinity for NO_2^-, while V_{max} denotes the maximum rate of NO_2^- oxidation that can be achieved under a particular set of conditions by a particular NOB community. In the ocean, direct measurements of NO_2^- oxidation kinetic parameters are extremely limited (Olson, 1981; Sun et al., 2017, 2021; Zhang et al., 2020), with no estimates available for the Southern Ocean. K_m values derived from culture studies of NOB range from 9-544 µM (Nowka et al., 2015; Ushiki et al., 2017), orders of magnitude higher than the existing estimates for natural assemblages of NOB in coastal waters and oxygen deficient zones (ranging from 0.07-0.51 µM; Olson, 1981; Sun et al., 2017; Zhang et al., 2020). This discrepancy emphasizes the gaps in our understanding of NO_2^- oxidation and the organisms that catalyse it.

Generally, NO_2^- concentrations in the low-latitude oxygenated ocean reach a maximum near the base of the mixed layer (i.e., the primary nitrite maximum; PNM), with much lower concentrations above and below this depth (Lomas and Lipschultz, 2006). By contrast, at higher latitudes including in the Southern Ocean, the NO_2^- concentrations are elevated (100-400 nM) and fairly invariant throughout the mixed layer in all seasons (Zakem et al., 2018; Fripiat et al., 2019; Mdutyana et al., 2020). A possible explanation for this NO_2^- accumulation is a decoupling of the NH_4^+ and NO_2^- oxidation rates, with NO_2^- oxidation being the rate-limiting step in the nitrification pathway, contrary to expectations for oxygenated marine waters (Kendall, 1998; Walker et al., 2010; Vajrala et al., 2013). However, this idea has yet to be examined using observations.

To better understand the controls on NO_2^- oxidation (and thus, nitrification) in the Southern Ocean, we conducted a series of NO_2^- oxidation kinetics experiments in wintertime surface waters across the western Indian sector. At every station (seven in total) along a transect between the Subtropical and Marginal Ice Zones, NO_2^- oxidation rates increased with increasing NO_2^- concentrations, as per the

https://doi.org/10.5194/bg-2021-280
Preprint. Discussion started: 29 October 2021

expected Michaelis-Menten relationship. The derived K_m values were low and increased with increasing ambient NO_2^-. Additionally, there appeared to be a minimum NO_2^- concentration that was required before the NO_2^- oxidation rates increased significantly, implying a "threshold" NO_2^- requirement of the enzyme that catalyses the oxidation of NO_2^- to NO_3^-. Finally, coincident measurements of euphotic zone NH_4^+ and NO_2^- oxidation rates suggest that NO_2^- oxidation is rate-limiting for nitrification across the Southern Ocean in winter.

2. Materials and Methods

2.1. Sampling site and experimental design

A winter cruise was undertaken onboard the R/V *SA Agulhas II* in July 2017 between Cape Town, South Africa, and the Marginal Ice Zone (MIZ; encountered at 61.7°S; de Jong et al., 2018), returning to South Africa along the meridional WOCE I06 transect (30ºE) (Figure 1). Sampling was conducted on two legs – between 37°S and 62°S on the southward leg (Leg 1) and between 59°S and 41°S on the return northward leg along the WOCE I06 line (Leg 2). During Leg 1, only surface samples were collected, while on Leg 2, the deployment of conductivity-temperature-depth (CTD) hydrocasts allowed for depth-profile sampling.

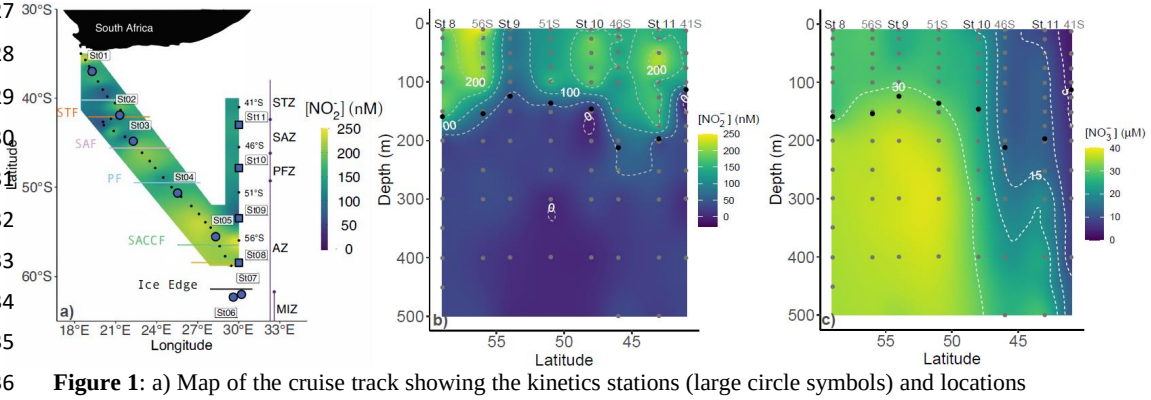

Figure 1: a) Map of the cruise track showing the kinetics stations (large circle symbols) and locations of the underway stations sampled during Leg 1 (small symbols), overlaid on the measured surface (~7 m) nitrite concentrations ($[NO_2^-]$). Additionally, the locations of the hydrocast stations occupied during Leg 2 are shown, with the stations at which depth-profile experiments were conducted shown by the large square symbols. The coloured horizontal lines denote the frontal positions at the time of sampling and the major zones of the Southern Ocean are indicated by the vertical lines and dots – STZ, Subtropical Zone; STF, Subtropical Front; SAZ, Subantarctic Zone; SAF, Subantarctic Front; PFZ, Polar Frontal Zone; PF, Polar Front; AZ, Antarctic Zone; SACCF, Southern Antarctic Circumpolar Front; MIZ, Marginal Ice Zone. Also shown are water column (0-500 m) profiles of the concentrations of b) nitrite (NO_2^-) and c) nitrate (NO_3^-) sampled during Leg 2. The vertical grey dots indicate the sampling depths at all the hydrocast stations (eight in total), with the four stations at which depth profile experiments were conducted (St 08 to St 11) labeled above the panel. The black dots show the mixed layer depths.

https://doi.org/10.5194/bg-2021-280
Preprint. Discussion started: 29 October 2021

150 *2.1.1 Hydrography and nutrient collections*: The positions of the major hydrographic fronts (the
151 Subtropical Front, STF; Subantarctic Front, SAF; Polar Front, PF; and Southern Antarctic Circumpolar
152 Current Front, SACCF; Figure 1) were determined from temperature and salinity measured by the ship's
153 hull-mounted thermosalinograph (~7 m), augmented by temperature, salinity, and oxygen
154 concentrations measured on Leg 2 by the CTD sensors (Orsi et al., 1995; Belkin and Gordon, 1996;
155 Pollard et al., 2002; Read et al., 2002). For the hydrocast stations, the mixed layer depth was determined
156 for each CTD (up)cast as the depth between 10 m and 400 m of maximum Brunt Väisälä frequency
157 squared (i.e., N^2) (Schofield et al., 2015; Carvalho et al., 2017).
158
159 *2.1.2 Nutrient samples*: Seawater samples were collected every four hours from the ship's underway
160 system (~7 m intake) on Leg 1 for the determination of NO_2^- concentrations (Figure 1a). During Leg 2,
161 samples were collected from Niskin bottles fired remotely between the surface and 500 m at eight
162 hydrocast stations for the analysis of NO_2^-, NO_3^-, and NH_4^+ concentrations (see Figure 1b and c for
163 station locations and sampling depths). For NO_2^- and NO_3^-, unfiltered seawater was collected in
164 duplicate 50 mL polypropylene centrifuge tubes that were analysed shipboard within 24 hours of
165 collection (NO_2^-) or stored frozen at -20°C until analysis (NO_3^-). Seawater samples for NH_4^+ were
166 collected unfiltered in duplicate high-density polyethylene (HDPE) bottles that had been "aged" with
167 orthophthaldialdehyde (OPA) working reagent, and analysed shipboard within 24 hours of collection.
168
169 *2.1.3 NO_2^- oxidation kinetics experiments*: On Leg 1, seawater samples were collected from the surface
170 via the ship's underway system at seven stations spanning the different zones of the Southern Ocean
171 (the Subtropical Zone (STZ) to the north of the STF, at the STF, the Subantarctic Zone (SAZ) between
172 the STF and SAF, the Polar Frontal Zone (PFZ) between the SAF and PF, the Open Antarctic Zone
173 (OAZ) between the PF and SACCF, and the Marginal Ice Zone (MIZ) south of the SACCF; St 01 to St
174 07 in Figure 1a). At each station, 25 L of seawater were collected in a single carboy that was gently
175 shaken to homogenize the contents before the seawater was filtered through a 200 µm nylon mesh to
176 remove zooplankton grazers and then dispensed into 250 mL acid-washed opaque HDPE bottles. All
177 the bottles were rinsed three times with sample water prior to filling. Eight sets of duplicate 250 mL
178 bottles were amended with $Na^{15}NO_2$ to yield $^{15}NO_2^-$ concentrations ranging from 10 nM to 1500 nM.
179
180 *2.1.4 Depth distribution of NO_2^- oxidation*: On Leg 2, seawater was collected at four stations (one each
181 in the Polar Antarctic Zone (PAZ; just north of the edge of the MIZ), OAZ, PFZ, and SAZ; St 08 to St
182 11 in Figure 1a-c) using a CTD-rosette equipped with 24 12-L Niskin bottles. Seawater from six depths
183 (10 m, 25 m, 50 m, 75 m, 200 m, and 500 m) was pre-filtered (200 µm nylon mesh) and transferred into
184 rinsed 250 mL acid-washed opaque HDPE bottles. Duplicate bottles from each depth were amended
185 with $Na^{15}NO_2$ to yield a final $^{15}NO_2^-$ concentration of 200 nM. From all incubation bottles (for kinetics
186 and depth-profile experiments), initial (T_0) subsamples were collected in 50 mL centrifuge tubes

https://doi.org/10.5194/bg-2021-280
Preprint. Discussion started: 29 October 2021


Biogeosciences Discussions Open Access EGU

immediately after the addition of $^{15}NO_2^-$. The HDPE bottles from the upper 75 m were then incubated in custom-built on-deck incubators supplied with running surface seawater, while those from 200 m and 500 m were incubated in a ~2ºC cold room. The incubations lasted 23-30 hours and were terminated via the collection of final (T_f) subsamples (50 mL). Subsamples were filtered (0.2 µm) and stored frozen at -20°C until analysis.

2.1.5 Depth distribution of NO_3^- uptake: To assess the extent to which mixed-layer NO_2^- oxidation supports wintertime NO_3^- uptake by phytoplankton, we also conducted NO_3^- uptake experiments over the upper 75 m (the approximate depth of the euphotic zone) at St 08 to St 11 on Leg 2. Seawater was collected from four depths – 10 m, 25 m, 50 m, and 75 m – in duplicate 2 L clear polycarbonate bottles following filtration (200 µm nylon mesh) to remove zooplankton grazers. $Na^{15}NO_3$ was added to each bottle to yield a final $^{15}NO_3^-$ concentration of 3 µM, and the bottles were then transferred to custom-built deck-board incubators equipped with neutral density screens that allowed for the penetration of 55%, 30%, 10%, and 1% of surface photosynthetically active radiation (PAR). The bottles were kept at near *in situ* temperature via a supply of continuously-running seawater from the underway system. Samples were incubated for 3-6 hours, and incubations were terminated by filtering the bottle contents through pre-combusted (450°C for 8 hours) 0.3 µm glass fibre filters (GF-75; Sterlitech) that were subsequently enclosed in foil envelops (pre-combusted at 500°C for 5 hours) that were stored at -80°C until analysis.

2.2. Laboratory analyses

2.2.1 Nutrient concentrations: Samples were analysed for NO_2^- concentrations onboard the ship using the colorimetric method of Grasshoff et al., (1983) and a Thermo Scientific Genesys 30 Visible spectrophotometer (detection limit of 20 nM, precision of ±20 nM). NO_3^-+NO_2^- concentrations were measured ashore using a Lachat Quick-Chem flow injection autoanalyzer (Egan, 2008) in a configuration with a detection limit of 0.2 µM and precision of ±0.3 µM. The concentration of NO_3^- was determined by subtracting NO_2^- from NO_3^-+NO_2^-. Aliquots of a certified reference material (JAMSTEC) were included in each NO_2^- and NO_3^-+NO_2^- run to ensure measurement accuracy. The NH_4^+ concentrations were also determined shipboard using the fluorometric method of Holmes et al. (1999); the methodological details and NH_4^+ data are discussed at length in (Mdutyana, 2021).

2.2.2 NO_2^- oxidation rates: Using the denitrifier-isotope ratio mass spectrometer (IRMS) method (Sigman et al., 2001; McIlvin and Casciotti, 2011), we measured the $\delta^{15}N$ of NO_3^- ($\delta^{15}N$-NO_3^-) produced from $^{15}NO_2^-$ oxidation for both the kinetics and depth-profile experiments ($\delta^{15}N$, in ‰ vs. air, = $(^{15}N/^{14}N_{sample}/^{15}N/^{14}N_{air} - 1) \times 1000$). Samples were measured using a Delta V Plus IRMS with a custom-built purge-and-trap front end (McIlvin and Casciotti, 2011) in a configuration with a detection limit of

https://doi.org/10.5194/bg-2021-280
Preprint. Discussion started: 29 October 2021


Biogeosciences Discussions Open Access EGU

223 0.2 nmol of N and a $\delta^{15}N$ precision of 0.2‰. Prior to isotope analysis, samples were treated with
224 sulfamic acid (15 mM) for 1 hour to remove $^{15}NO_2^-$ remaining at the end of the experiments, after which
225 sample pH was adjusted to ~7-8 via the addition of 2 M NaOH. To account for inefficiencies in $^{15}NO_2^-$
226 removal, both the T_f and T_0 samples were treated with sulfamic acid and analysed for $\delta^{15}N\text{-}NO_3^-$ (more
227 accurately, $\delta^{15}N\text{-}NO_3^- + NO_2^-$), with the difference between them taken as the $^{15}NO_3^-$ enrichment due to
228 $^{15}NO_2^-$ oxidation (Peng et al., 2015). International reference materials (IAEA-N3, USGS 34, USGS 32)
229 were used to calibrate the measured $\delta^{15}N\text{-}NO_3^-$.
230
231 The rate of NO_2^- oxidation ($NO_2^-{}_{ox}$; nM d^{-1}) was calculated following Peng et al., (2015) as:
232
233 $$NO_2^-{}_{ox} = \frac{\Delta[^{15}NO_3^-]}{f_{NO_2^-}^{15} \times T} \quad (1)$$
234
235 Where $\Delta[^{15}NO_3^-]$ is the change in the concentration of $^{15}NO_3^-$ between the start and end of the incubation
236 due to NO_2^- oxidation, calculated from the difference in the measured $\delta^{15}N\text{-}NO_3^-$ between the T_f and T_0
237 samples, $f_{NO_2^-}^{15}$ is the fraction of the NO_2^- substrate pool labelled with ^{15}N at the start of the incubation,
238 and T is the incubation length (days). Detection limits for $NO_2^-{}_{ox}$ rates ranged from 0.11 to 0.36 nM d^{-1}, calculated according to Santoro et al., (2013) and Mdutyana et al., (2020).
240
241 *2.2.3 Kinetic model:* Kinetic parameters are typically calculated using the Michaelis-Menten (MM)
242 equation for enzyme kinetics (Monod, 1942):
243
244 $$V = \frac{V_{max} \times S}{K_m + S} \quad (2)$$
245
246 where V is the measured reaction rate, V_{max} is the maximum reaction rate achievable under *in situ*
247 conditions at saturating substrate (S) concentrations, and K_m is the half-saturation constant, defined as
248 the substrate concentration at which $V = V_{max}/2$.
249
250 The MM equation (equation 2) is a rectangular hyperbola, meaning that the asymptotes along the x-
251 and y-axes are perpendicular. By definition, when S (the x-axis variable) is equal to zero, V (the y-axis
252 variable) is also zero, forcing the model through the origin (0,0). In the case of NO_2^- oxidation, the
253 assumption that once $S > 0$, $V > 0$ is appropriate in waters where the ambient NO_2^- concentration is
254 near-zero or where NO_2^- is non-zero but considerably lower than the K_m. In the Southern Ocean, mixed-
255 layer NO_2^- concentrations are typically always ≥150 nM (Cavagna et al., 2015; Zakem et al., 2018;
256 Fripiat et al., 2019; Mdutyana et al., 2020) and forcing the MM model through the origin results in a

https://doi.org/10.5194/bg-2021-280
Preprint. Discussion started: 29 October 2021

poor fit to the measurements (red line in Figure S1). This poor fit, in turn, leads to clearly inaccurate estimates of the kinetic parameters, particularly K_m (Table S1).

While not typical for studies of NO_2^- oxidation kinetics in the ocean, the standard form of non-linear regression models, including the MM equation, can be modified to better fit observations (e.g., Birch, 1999; Tsoularis and Wallace, 2002; Archontoulis and Miguez, 2014). For application to our dataset, we modified equation 2 to allow V = 0 at S > 0 by subtracting a location parameter, C, from S (Figure 2; Archontoulis and Miguez, 2014). In other words, we set the y-intercept (i.e., where V = 0) equal to C rather than to zero, which yields equation 3:

$$V = \frac{V_{max} \times (S-C)}{K_{m*} + (S-C)} \quad (3)$$

Using a non-linear, least-squares optimization method (Scipy lmfit package, Python 3.7.6), we solved equation 3 for V_{max}, K_{m*}, and C. The value of K_{m*} derived thus is relative to C, such that the substrate concentration at which $V = V_{max}/2$ (i.e., K_m) is actually equal to $K_{m*} + C$ (Supplemental Information). Mechanistically, C represents a "threshold" substrate concentration; when $S \leq C$, V = 0. All kinetic parameters are reported as the best fit plus 95% confidence interval (i.e., mean ± 2σ; Table 1).

2.2.4 Revising the depth distribution of NO_2^- oxidation using K_m: For the NO_2^- oxidation experiments conducted at the Leg 2 hydrocast stations (i.e., depth-profile experiments; St 08 to St 11), the $Na^{15}NO_2$ was added to yield a final $^{15}NO_2^-$ concentration of 200 nM at all the sampled depths. However, at low ambient NO_2^- concentrations (<1-2 μM), an amendment of this magnitude may stimulate NO_2^- oxidation, leading to an overestimation of the *in situ* rates. We thus revised our measured $NO_2^-{}_{ox}$ rates using the derived K_m values as per Rees et al., (1999), Diaz and Raimbault, (2000), and Horak et al., (2013):

$$\mathrm{corrNO_{2_{Ox}}^-} = \frac{\mathrm{NO_{2_{Ox}}^-}}{\frac{[\mathrm{NO_2^-}]_{total}}{K_m + [\mathrm{NO_2^-}]_{total}} \times \frac{K_m + [\mathrm{NO_2^-}]_{amb}}{[\mathrm{NO_2^-}]_{amb}}} \quad (4)$$

Here, $corrNO_2^-{}_{ox}$ is the revised rate of $NO_2^-{}_{ox}$, $NO_2^-{}_{ox}$ is the measured NO_2^- oxidation rate (equation 1), $[NO_2^-]_{amb}$ is the ambient NO_2^- concentration measured at each depth, $[NO_2^-]_{total}$ refers to the [$^{15}NO_2^-$ tracer] + $[NO_2^-]_{amb}$, and K_m is the derived half-saturation constant. We estimated a K_m for each sample depth from the equation resulting from the linear regression of all derived K_m values on $[NO_2^-]_{amb}$ (see section 4.2 below). We also computed $corrNO_2^-{}_{ox}$ using the K_m derived from the Leg 1 kinetics experiment located nearest each hydrocast station, which yielded very similar results. The values of $corrNO_2^-{}_{ox}$ presented here were computed using the K_m values derived from the linear regression

https://doi.org/10.5194/bg-2021-280
Preprint. Discussion started: 29 October 2021

292 equation. Rates of NH_4^+ oxidation measured coincident with $NO_2^-{}_{ox}$ on Leg 2 (see Mdutyana 2021) were
293 similarly revised (to yield $corrNH_4^+{}_{ox}$) using the K_m values derived from kinetics experiments conducted
294 during Leg 1 – for St 08 and 09, K_m =137 nM, for St 09, K_m = 67 nM, and for St 11, K_m = 28 nM.
295
296 *2.2.5 Isotopic dilution of $^{15}NO_2^-$ by co-occurring NH_4^+ oxidation:* The focus of this study is the second
297 step in the nitrification pathway. However, not only will NO_2^- have been consumed in our incubation
298 bottles (i.e., oxidized to NO_3^-), but it will also have been produced by NH_4^+ oxidation, the first step in
299 the nitrification pathway. For all of our NO_2^- oxidation rate experiments (kinetics and depth-profile),
300 we measured the coincident rates of NH_4^+ oxidation (Mdutyana, 2021), and these data can be used to
301 account for any dilution of the $^{15}NO_2^-$ pool by $^{14}NO_2^-$ produced from $^{14}NH_4^+$ oxidation (following the
302 approach of Glibert et al., 1982, 1985; Mulholland and Bernhardt, 2005). We found that isotopic
303 dilution in the mixed layer was minor because the ambient NO_2^- concentrations were reasonably high
304 (mean of 157 ± 54 nM, range of 64 to 226 nM for all the depths at which experiments were conducted;
305 Figure 1a-b) and the NH_4^+ oxidation rates were fairly low (mean of 13.4 ± 4.0 nM d^{-1}, range of 7.8 to
306 22.0 nM d^{-1}; see Figure 3f-j for the depth profile rates and Mdutyana (2021) for the kinetics station
307 rates). Below the mixed layer where the ambient NO_2^- concentrations were near-zero, so too were the
308 NH_4^+ oxidation rates, which again resulted in minimal dilution of the $^{15}NO_2^-$ pool. Accounting for
309 isotope dilution increased the NO_2^- oxidation rates by 0 to 12% (mean of 3.9 ± 0.3% and median of 3.7
310 ± 0.3%), which is within the experimental error associated with the rate measurements; we thus consider
311 the effect of isotope dilution to be negligible
312
313 *2.2.6 Nitrate uptake rates*: On shore, the GF-75 filters were oven-dried at 45°C for 24 hours, then
314 pelletized into tin cups following the removal of unused peripheral filter. The concentration and isotopic
315 composition of the particulate organic N (PON) captured on the filters was analyzed using a Delta V
316 Plus IRMS coupled to a Flash 2000 elemental analyser, with a detection limit of 1 µg N and precision
317 of ±0.005 At%. Blanks (combusted unused filters + tin capsules) and laboratory running standards
318 calibrated to international reference materials were run after every five to ten samples. The absolute
319 rates of NO_3^- uptake (ρNO_3^-; nM d^{-1}) were calculated after blank correction according to the equations
320 of Dugdale and Wilkerson (1986) assuming a day-length of between 7 and 10 hours, depending on the
321 station latitude. To compute the fraction of the mixed-layer NO_3^- pool consumed by phytoplankton that
322 derived from *in situ* nitrification, we trapezoidally-integrated ρNO_3^- and $corrNO_2^-{}_{ox}$ over the mixed layer
323 following Mdutyana et al., (2020), and then divided the integrated values of $corrNO_2^-{}_{ox}$ by ρNO_3^-.
324
325 **3. Results**
326
327 3.1 Hydrography and nutrient concentrations

https://doi.org/10.5194/bg-2021-280
Preprint. Discussion started: 29 October 2021

328 The positions of the major hydrographic fronts during both legs of the cruise are shown in Figure 1a.
329 At the hydrocast stations (Leg 2), the mixed layer depth (MLD) averaged 143 m in the OAZ, 146 m in
330 the PFZ, 205 m in the SAZ, and 113 m in the STZ, which is within the reported climatological range
331 for the western Indian sector in winter (Sallée et al. 2010). Underway ambient NO_2^- concentrations (Leg
332 1) ranged from 74 nM to 232 nM (transect average of 168 ± 48 nM, median of 177 nM) and generally
333 increased with latitude, albeit with a high degree of variability (Figure 1a; Figure S2). The ambient NO_2^-
334 concentrations at the hydrocast stations were fairly constant throughout the mixed layer (ranging from
335 55 ± 35 nM to 159 ± 73 nM), decreasing rapidly to values below detection by 150-200 m (Figure 1b).
336 Mixed-layer NO_2^- showed no clear latitudinal trend, mainly because of the anomalously low
337 concentrations measured at St 09 (54°S; mixed-layer average of 64 ± 30 nM, compared to 144 ± 56 for
338 the seven other hydrocast stations). The NO_3^- concentrations were also near-homogenous throughout
339 the mixed layer, decreasing from an average of 28.4 ± 0.2 µM at the southernmost station (St 08; 59°S)
340 to 3.7 ± 1.1 µM at the northernmost station (41°S), and increasing below the mixed layer as expected
341 (Figure 1c).
342
343 3.2. NO_2^- oxidation rates
344 *3.2.1 Kinetics experiments*: At all the kinetics stations (St 01 to St 07; Leg 1), an MM curve could be
345 fit to the NO_2^- oxidation rate *versus* substrate concentration measurements using equation 3 (Figure 2).
346 The derived kinetic parameters varied across the transect (Table 1). The maximum NO_2^- oxidation rate
347 (V_{max}) increased southwards from from 5.2 ± 0.1 nM d^{-1} at the STF (St 02; Figure 2b) to 13 ± 0.4 nM
348 d^{-1} in the AZ (St 05; Figure 2e), before decreasing in the MIZ to 8.2 ± 0.1 nM d^{-1} at St 06 (Figure 2f)
349 and 6.6 ± 0.3 nM at St 07 (Figure 2g). The average V_{max} for the transect was 9.0 ± 1.1 nM d^{-1}. The half-
350 saturation constant, K_m, increased from 134 ± 8.0 nM at the STF (St 02) to 403 ± 24 nM in the MIZ (St
351 06), with a transect average of 277 ± 31 nM. The value of C showed a positive relationship with $[NO_2^-]_{amb}$
352 and no strong relationship with latitude, and ranged from 115 ± 2.3 nM at the STF (St 02) to 245 ±
353 18 nM in the A Z (St 05), with a transect average of 181 ± 45 nM.

Table 1: Kinetic parameters (V_{max}, K_m and C) associated with NO_2^- oxidation experiments conducted across the western Indian sector of the Southern Ocean in winter 2017. Included here is the best fit and 95% confidence interval ("CI") for each kinetic parameter, derived using a non-linear, least-squa7res optimization method (Scipy lmfit package, Python 3.7.6).

Station name	Latitude	Longitude	$[NO_2^-]_{amb}$ (nM)	V_{max} (nM d^{-1})	95%CI (nM d^{-1})	K_m (nM)	95%CI (nM)	C (nM)	95%CI (nM)
St 01	37°S	19°E	157	9.1	7.9 to 10	263	192 to 350	193	144 to 206
St 02	42°S	21°E	108	5.2	4.8 to 5.5	134	109 to 163	115	105 to 119
St 03	45°S	22°E	103	8.3	7.4 to 9.3	206	15 to 373	139	-11 to 163
St 04	50°S	26°E	162	13	11 to 15	288	104 to 538	172	68 to 204
St 05	55°S	28°E	212	14	13 to 15	329	183 to 458	245	138 to 272
St 06	62°S	30°E	226	8.2	7.8 to 8.6	403	320 to 499	163	129 to 187
St 07	62°S	30°E	226	6.6	6.0 to 7.4	317	234 to 395	237	190 to 255

https://doi.org/10.5194/bg-2021-280
Preprint. Discussion started: 29 October 2021

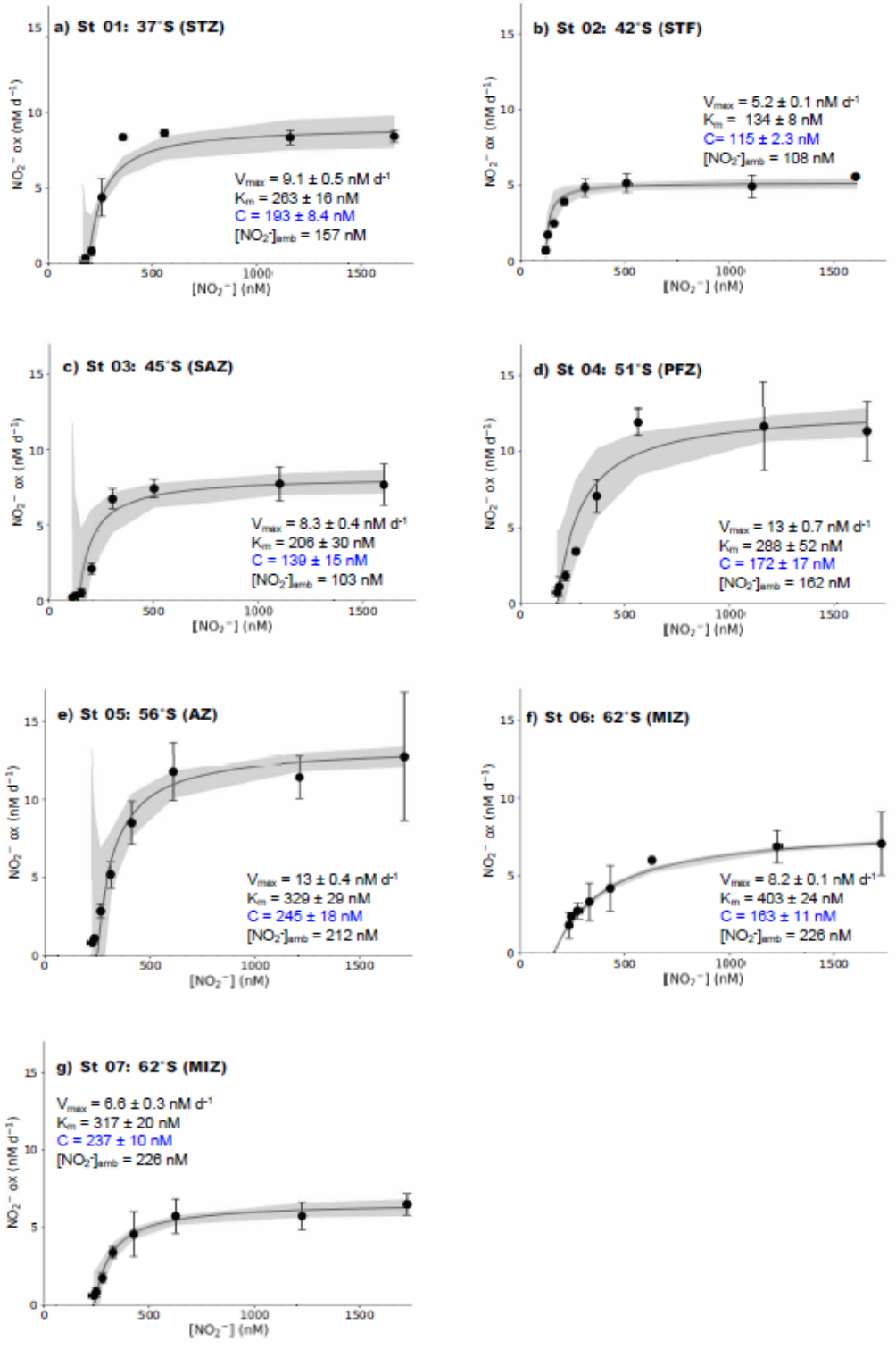

https://doi.org/10.5194/bg-2021-280
Preprint. Discussion started: 29 October 2021

Figure 2: Kinetics experiments: the dependence of NO_2^- oxidation rates on NO_2^- concentration ([NO_2^-]) at the surface (~7 m) in winter at a) St 01: 37°S (STZ), b) St 02: 42°S (STF), c) St 03: 45°S (SAZ), d) St 04: 51°S (PFZ), e) St 05: 55°S (OAZ), f) St 06: 62°S (MIZ), and g) St 07: 62°S (MIZ). The solid lines show the Michaelis-Menten best fit, with the derived values of V_{max}, K_m, and C, as well as the ambient concentration of nitrite ($[NO_2^-]_{amb}$), indicated on each panel. Error bars indicate the standard error of replicate experiments, each measured at least twice. Where errors bars are not visible, they are smaller than the data markers. The grey shaded area shows the 95% confidence interval associated with the model fit. Note that the x-axis represents total [NO_2^-] (i.e., [$^{15}NO_2^-$ tracer] + $[NO_2^-]_{amb}$).

3.2.2 Depth-profile experiments: NO_2^- oxidation rates at St 08 to St 11, calculated using equation 1, were low and largely invariant over the upper 75 m, ranging from 1.9 to 9.7 nM d^{-1} (average of 4.9 ± 2.4 nM d^{-1}; filled symbols in Figure 3b-e). All stations showed a maximum NO_2^- oxidation rate at 200 m (roughly coincident with or just below the base of the mixed layer), ranging between 11 and 28 nM d^{-1} (average of 18 ± 7.0 nM d^{-1}). The NO_2^- oxidation rates showed a latitudinal gradient, with lower rates in the AZ (St 08 and 09) than in the PFZ (St 10) and SAZ (St 11).

Revising the NO_2^- oxidation rates using equation 4 decreased their 0-75 m values by 13 to 26% (i.e., $corrNO_2^-{}_{ox}$ ranged from 1.6 to 8.5 nM d^{-1} and averaged 4.0 ± 2.0 nM d^{-1} over the upper 75 m; open symbols in Figure 3b-e). The largest decrease (of 39 to 68%) occurred at 200 m and 500 m, coinciding with very low ambient NO_2^- concentrations (Figure 3a); nonetheless, at all but St 08, the maximum NO_2^- oxidation rate was still observed at 200 m, although its magnitude was lower. The coincidentally-measured and revised NH_4^+ oxidation rates ($corrNH_4^+{}_{ox}$) showed a similar pattern, with the largest decrease occurring at the depths with the lowest ambient NH_4^+ concentrations (Figure 3f-j) – over the upper 75 m, the rates decreased by 1 to 9% at St 08 to St 10 where the mixed-layer ambient NH_4^+ concentrations averaged 263 ± 4.3 to 655 ± 15 nM, while at St 11 where the mixed-layer ambient NH_4^+ concentration averaged 13 ± 1.6 nM, the rates decreased by 40 ± 23%. Similar to the NO_2^- oxidation rates, the NH_4^+ oxidation rates decreased most at 200 m and 500 m, between 33% and 70%. Hereafter, we use the revised NO_2^- and NH_4^+ oxidation rates ($corrNO_2^-{}_{ox}$ and $corrNH_4^+{}_{ox}$, respectively) when referring to the depth distributions of these processes, including in Figures 5 and 6. We note, however, that the revised rates may still not be entirely accurate since K_m was not derived individually for each depth at each station (Horak et al., 2013). Nonetheless, because of the high concentration of the ^{15}N-tracer amendments relative to all derived K_m values, we are confident that the revised rates are more representative of *in situ* conditions than the rates computed using equation 1.

https://doi.org/10.5194/bg-2021-280
Preprint. Discussion started: 29 October 2021

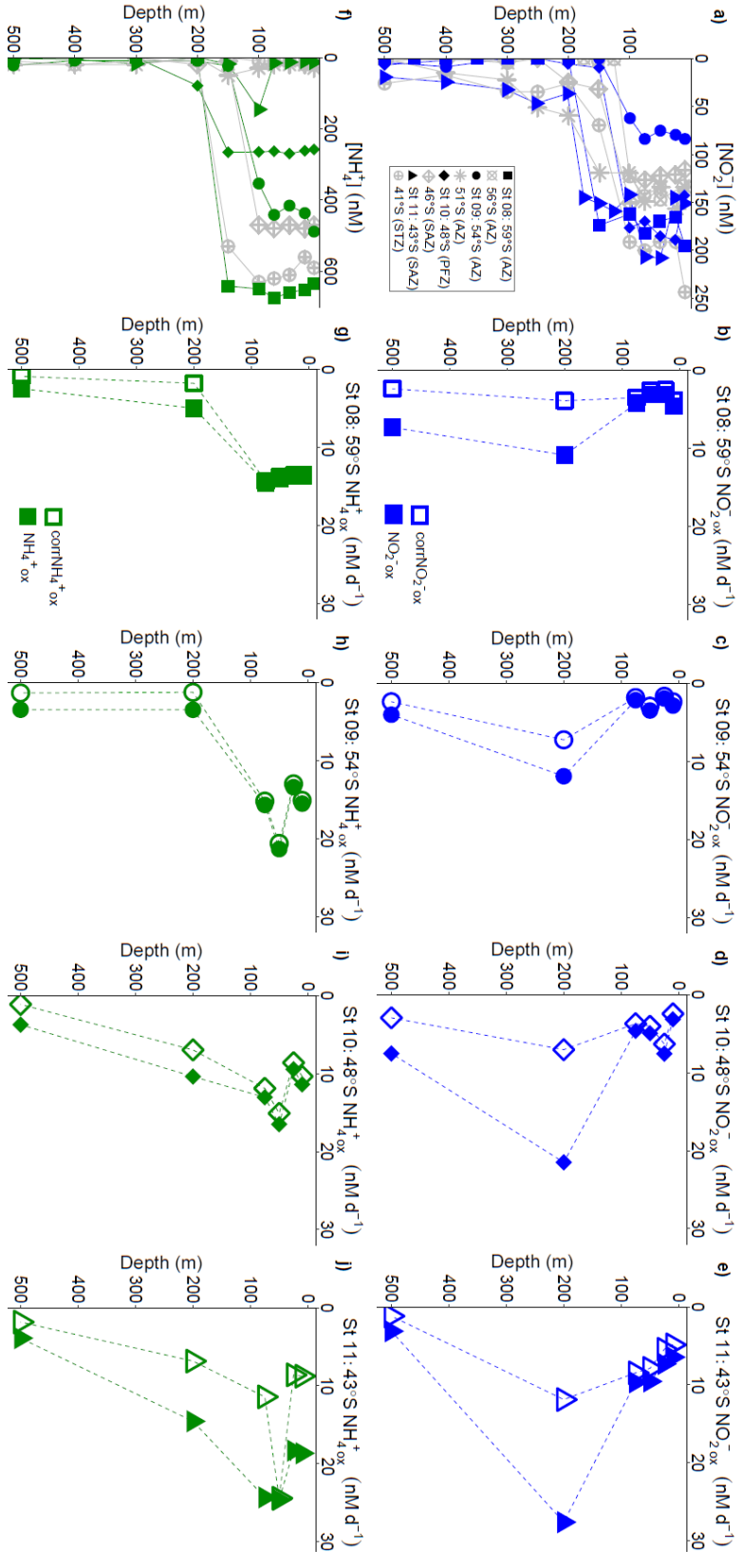

Figure 3: Depth-profile experiments: water column (0-500 m) profiles of the concentration of a) nitrite ($[NO_2^-]$) and f) ammonium ($[NH_4^+]$), and rates of NO_2^- and NH_4^+ oxidation at b and g) St 08: 59°S (AZ), c and h) St 09: 54°S (AZ), d and i) St 10: 48°S (PFZ), and e and j) St 11: 43°S (SAZ). In panels a and f, the blue and green symbols indicate the stations at which oxidation rates were measured while the grey symbols show data from the stations where no experiments were conducted. In panels b-e and g-j, open symbols represent oxidation rates revised for possible stimulation due to ^{15}N-tracer additions ($corrNO_2^-{}_{ox}$ and $corrNH_4^+{}_{ox}$; equation 4) and closed symbols show the uncorrected rates (equation 1). Error bars indicate the standard error of replicate experiments, each measured at least twice. Where error bars are not visible, they are smaller than the data markers. The dashed lines connecting the data points are included only to guide the eye and should not be taken to indicate interpolation with depth.

https://doi.org/10.5194/bg-2021-280
Preprint. Discussion started: 29 October 2021

3.3 NO_3^- uptake rates

The rates of NO_3^- uptake (ρNO_3^-) were low and relatively homogenous over the upper 75 m at each station (Figure S3a). Average euphotic zone ρNO_3^- increased northwards, from 2.9 ± 1.1 nM d^{-1} at St 08 in the AZ to 12 ± 2.0 nM d^{-1} at St 11 in the SAZ, with a transect average of 6.2 ± 3.4 nM d^{-1}. The euphotic zone PON concentrations also increased northwards, from 0.24 ± 0.02 µM at St 08 to 0.47 ± 0.08 µM at St 11 (Figure S3b).

Integrated over the mixed layer, $corrNO_2^-{}_{ox}$ accounted for an average of 122% of ρNO_3^- (range of 63% at St 09 to 237% at St 08 in the AZ; Table S2), as has been observed previously in the wintertime Southern Ocean (Mdutyana et al., 2020). These data confirm that, at least in a mass balance sense, most of the mixed-layer NO_3^- consumed by phytoplankton in winter, and likely also a significant fraction assimilated in spring, supports regenerated rather than new production, thus weakening the biological CO_2 sink and complication the use of new production as a proxy for carbon export (Yool et al., 2007; Mdutyana et al., 2020).

4. Discussion

NO_2^- oxidation, the ultimate step in the nitrification pathway, is important in oceanic N cycling because it produces NO_3^-, the most oxidized and dominant form of N that controls phytoplankton growth across most of the global ocean (Moore et al., 2013). Experiments designed to measure the kinetics of NO_2^- oxidation, as conducted here, allow for an examination of the controls on marine nitrification. Across all the major zones of the wintertime Southern Ocean, the addition of NO_2^- to samples of surface seawater stimulated NO_2^- oxidation following a Michaelis-Menten relationship, suggesting that substrate availability plays a dominant role in determining the rate of NO_3^- production in the Southern Ocean's winter mixed layer. Curiously, however, we also observed an apparent minimum substrate requirement of NO_2^- oxidation (i.e., a "threshold" NO_2^- concentration, ranging from 115 to 245 nM), which is in contrast to expectations for a "classical" Michaelis-Menten relationship (i.e., V is assumed to increase as soon as S > 0, assuming S is limiting to V; Monod, 1942). Below, we examine our findings in the context of existing estimates of NO_2^- oxidation kinetic parameters and then evaluate the potential drivers of the trends that we observe. We also discuss possible reasons for the apparent requirement of Southern Ocean NOB for a threshold ambient NO_2^- concentration and consider the implications thereof for the regional N cycle.

4.1 Southern Ocean NO_2^- oxidation kinetic parameters in the context of existing estimates

Measurements of NO_2^- oxidation rates are limited in the Southern Ocean, with only two studies that have directly measured this pathway in open-ocean waters (Bianchi et al., 1997; Mdutyana et al., 2020). For NO_2^- oxidation kinetics, there are no data at all for the Southern Ocean. This scarcity of measurements is unsurprising given that *in situ* NO_2^- oxidation kinetics studies are generally limited;

https://doi.org/10.5194/bg-2021-280
Preprint. Discussion started: 29 October 2021

indeed, to our knowledge, there are only two studies from the coastal ocean (Olson, 1981a; Zhang et al., 2020) and two from the Eastern Tropical North Pacific oxygen deficient zone (ETNP ODZ; with experiments conducted across a range of ambient oxygen concentrations; Sun et al., 2017, 2021). By contrast, there exist numerous estimates of NO_2^- oxidation kinetic parameters determined from studies using cultured marine NOB (e.g., Sorokin et al., 2012; Nowka et al., 2015; Jacob et al., 2017; Kits et al., 2017; Zhang et al., 2020). In general, culture experiments suggest far higher kinetic constants compared to the limited *in situ* observations from the ocean, particularly for K_m (i.e., culture-based estimates of 9-544 µM; Blackburne et al., 2007; Nowka et al., 2015; Ushiki et al., 2017).

The high K_m values derived for cultured NOB suggest that the affinity of these organisms for NO_2^- is low. However, this is not what is observed in the environment, which indicates that the most abundant NOB in the ocean are not represented in the culture collection. For the Southern Ocean, we report high substrate affinities of NOB, with K_m values ranging from 134 to 403 nM, which is largely within the range documented for coastal waters (27-506 nM; Zhang et al., 2020) and the oxygenated open ocean (27-506 nM; Olson, 1981; Zhang et al., 2020) (Table 2). In the low- to zero-oxygen waters of the ETNP ODZ, similarly low K_m values have been reported (254 ± 161 nM; Sun et al., 2017), as have values >5 µM (Sun et al., 2021). These latter estimates were associated with ambient NO_2^- concentrations >1 µM. We explore the relationship between ambient NO_2^- concentration and K_m in detail in section 4.2 below. Our focus is on the K_m values derived under conditions of low ambient NO_2^- given that (some of) the environmental factors affecting NO_2^- oxidation at high ambient NO_2^- concentrations appear to be unique. For example, oxygen has been shown to decrease the rate of NO_2^- oxidation in the ODZs (Sun et al., 2017, 2021) where novel clades of NOB have been detected (Sun et al., 2021).

Table 2: A selection of previously derived K_m values from various regions of the open ocean, along with the concurrently-measured ambient concentrations of nitrite ($[NO_2^-]_{amb}$). The numbers in parenthesis are standard errors.

Region	$[NO_2^-]$ (nM)	Sampled depth (m)	Km (nM)	Reference
Indian Southern Ocean: St 01: 37°S	157	7	263 (16)	This study
Indian Southern Ocean: St 02: 42°S	108	7	134 (8)	This study
Indian Southern Ocean: St 03: 45°S	103	7	206 (30)	This study
Indian Southern Ocean: St 04:51°S	162	7	288 (52)	This study
Indian Southern Ocean: St 05: 56°S	212	7	329 (29)	This study
Indian Southern Ocean: St 06: 62°S	226	7	403 (24)	This study
Indian Southern Ocean: St 07: 62°S	226	7	317 (20)	This study
Southern California Bight	20	60	70	Olson 1981
Eastern Tropical North Pacific	100	53	281 (151)	Sun et al. 2017
Eastern Tropical North Pacific	50	170	227 (55)	Sun et al. 2017
South China Sea	51	110	195 (33)	Zhang et al. 2020
South China Sea	71	95	175 (37)	Zhang et al. 2020
South China Sea	31	150	49 (15)	Zhang et al. 2020
South China Sea	185	75	506 (82)	Zhang et al. 2020
South China Sea	34	200	27 (11)	Zhang et al. 2020
Subtropical South Atlantic	14	150	74 (29)	Fawcett et al. in prep
Subtropical South Atlantic	152	150	167 (4.3)	Fawcett et al. in prep

https://doi.org/10.5194/bg-2021-280
Preprint. Discussion started: 29 October 2021

505 Across our Southern Ocean transect, V_{max} ranged from 5 to 14 nM d^{-1}, which is relatively low compared
506 to estimates from other regions (Table 2), although such a comparison may not be particularly
507 informative as our rates (and typically those of others) are not normalized for NOB abundance. Our
508 V_{max} estimates are also low compared to a previous study of mixed-layer nitrification in the winter
509 Southern Ocean (Mdutyana et al., 2020). This difference may in part be due to the fact that the kinetics
510 experiments were conducted using surface (~7 m) seawater (and thus, the surface NOB community that
511 had been exposed to surface conditions, including elevated light), yet the highest rates of NO_2^- oxidation
512 often occur near the base of the mixed layer, including in the Southern Ocean (Figure 3b-e; Sun et al.,
513 2017; Peng et al., 2018; Mdutyana et al., 2020). The opposite pattern has also been observed, however,
514 with deeper samples yielding a lower V_{max} than samples collected in shallow waters (Sun et al., 2017;
515 Zhang et al., 2020).
516
517 4.2 Environmental drivers of the NO_2^- oxidation kinetic parameters
518 We report maximum NO_2^- oxidation rates that generally increase towards the south and with decreasing
519 SST (recognizing that these parameters co-vary), although St 01 in the STZ and St 06 and 07 in the
520 MIZ deviate from this trend (Figure 4a and b; $R^2 = 0.019$; $p = 0.77$ and $R^2 = 0.12$; $p = 0.45$, respectively
521 when all the stations are considered, and $R^2 = 0.92$; $p = 0.041$ and $R^2 = 0.94$; $p = 0.029$, respectively,
522 when St 01, 06, and 07 are excluded). It is possible that changes in the NOB community (composition
523 and/or abundance) across the transect explains some of the observed variability. Nonetheless, taking
524 latitude as a qualitative proxy for light, it is perhaps unsurprising that the maximum NO_2^- oxidation
525 rates increase southwards given that NOB are known to be at least partially light inhibited (Peng et al.,
526 2018; Ward, 2005; Olson, 1981b). This hypothesis does not hold for the stations in the MIZ, however,
527 at which V_{max} decreases sharply despite these waters receiving the least light (less than 5 hours of weak
528 sunlight, versus ~7 hours at 55ºS to ~9 hours at 37ºS). The temperature at the MIZ stations was <0°C,
529 which raises the possibility of a temperature effect on V_{max}. Indeed, we previously observed a strong
530 decline in the V_{max} associated with NH_4^+ oxidation at SSTs <0°C in the Southern Ocean, while at SSTs
531 ranging from 0.6°C to 16°C, V_{max} was near invariant (Mdutyana, 2021).
532
533 Marine nitrification has been reported to be largely unaffected by temperature variations (Bianchi et al.,
534 1997; Horak et al., 2013; Baer et al., 2014), although NH_4^+ and NO_2^- oxidation may respond differently
535 to similar changes in temperature. For example, marine NOB incubated at temperatures ranging from
536 10°C to 35°C responded far more slowly to an increase in temperature than co-incubated AOA, resulting
537 in an accumulation of NO_2^- in the incubation bottles (Schaefer and Hollibaugh, 2017). By contrast, we
538 previously observed no robust relationship between temperature and the maximum NH_4^+ oxidation rate
539 in the Southern Ocean (Mdutyana, 2021), a finding that is consistent with studies of NH_4^+ oxidation in
540 the Arctic and temperate coastal ocean (Horak et al., 2013; Baer et al., 2014). Far less work has been
541 done to assess the response of NOB to temperature changes. In the absence of experiments specifically

https://doi.org/10.5194/bg-2021-280
Preprint. Discussion started: 29 October 2021

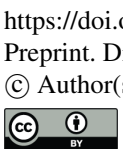

designed to test the response of Southern Ocean NOB communities to temperature, it is difficult to disentangle the effect(s) on NO_2^- oxidation of temperature *versus* light (and possibly other parameters that co-vary with latitude, such as NO_2^- and/or micronutrient availability).

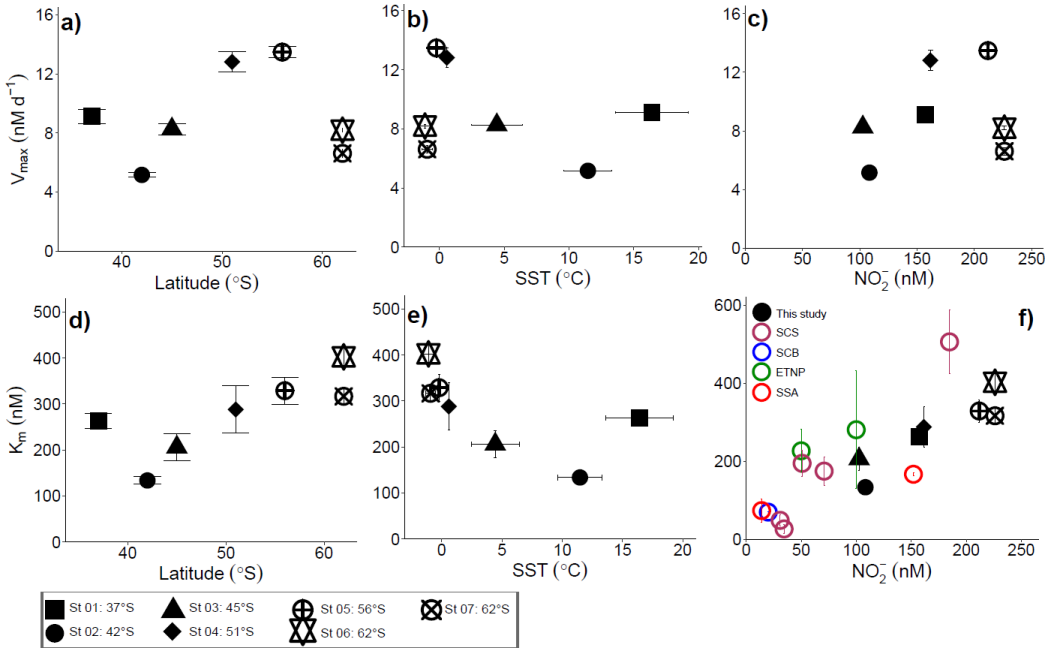

Figure 4: Potential controls on the kinetic parameters associated with NO_2^- oxidation. V_{max} and K_m are shown as a function of a and d) latitude, b and e) sea surface temperature (SST), and c and f) the ambient nitrite concentration ($[NO_2^-]_{amb}$). Vertical error bars show the propagated error associated with V_{max} and K_m computed using a non-linear, least-squares optimization method (Scipy lmfit package, Python 3.7.6), while the symbols and horizontal error bars on panels b and e indicate the average (± standard deviation) SST experienced by the samples during the incubations. In panel f, black symbols show our Southern Ocean data, maroon symbols show K_m values from the South China Sea (SCS; Zhang et al. 2020), the blue symbol shows the K_m value derived for the South California Bight (SCB; Olson 1981a), the green symbol shows K_m values from Eastern Tropical North Pacific oxygen deficient zone (ETNP; Sun et al. 2017), and the red symbols show K_m values derived for the subtropical southeast Atlantic (SSA; Fawcett et al. unpubl.).

Plotting V_{max} as a function of the ambient substrate concentration ($[NO_2^-]_{amb}$) reveals a strong positive relationship for all but the MIZ stations (Figure 4c; R^2 = 0.73; p = 0.065 if the MIZ stations are excluded). In particular, the STZ station (St 01), which appeared anomalous in the plots of V_{max} versus latitude and SST, is consistent with the other non-MIZ stations when evaluated in V_{max} versus $[NO_2^-]_{amb}$ space. The positive relationship of V_{max} to $[NO_2^-]_{amb}$ could be taken as evidence that NO_2^- availability strongly controls the maximum achievable rate of NO_2^- oxidation. However, V_{max} varies four-fold across the transect while $[NO_2^-]_{amb}$ only changes by a factor of two, and $[NO_2^-]_{amb}$ is also correlated with latitude (R^2 = 0.51, p = 1.1x10^{-5} for all surface $[NO_2^-]_{amb}$ data; Figure S2). Additionally, previous wintertime Southern Ocean NO_2^- oxidation rates (albeit not V_{max}) showed no relationship with ambient

https://doi.org/10.5194/bg-2021-280
Preprint. Discussion started: 29 October 2021

567 NO_2^- concentration (Bianchi et al., 1997; Mdutyana et al., 2020). The extent to which V_{max} is directly
568 controlled by $[NO_2^-]_{amb}$ is thus unclear, and it is likely that NOB community composition, light
569 availability, and temperature also play a role, with SST perhaps becoming more important at very low
570 temperatures (i.e., in the MIZ).
571
572 Our estimates of K_m reveal that NOB in the wintertime Southern Ocean have a high affinity for NO_2^-
573 that appears to decrease (i.e., the K_m rises) at higher latitudes (i.e., lower light) and lower temperatures,
574 with St 01 in the STZ again emerging as an exception (Figure 4d and e; $R^2 = 0.86$, $p = 0.0075$ and $R^2 =$
575 0.86, $p = 0.0076$, respectively). Plotting our K_m values as a function of $[NO_2^-]_{amb}$ reveals a strong
576 positive relationship (Figure 4f; $R^2 = 0.83$, $p = 0.0044$; black data points), implying that NO_2^- availability
577 rather than temperature or light exerts the dominant control on K_m. This trend further suggests that NOB
578 are well-adapted to the environment (or Southern Ocean region) in which they are found. Southern
579 Ocean mixed-layer NO_2^- concentrations are almost never <150 nM, regardless of the season (Fripiat et
580 al., 2019; Mdutyana et al., 2020; Zakem et al., 2018), yet the relationship of K_m to $[NO_2^-]_{amb}$ also holds
581 at far lower NO_2^- concentrations. The coloured data points in Figure 4f show K_m versus $[NO_2^-]_{amb}$ for
582 four additional regions where a Michaelis-Menten relationship of NO_2^- oxidation rate to NO_2^-
583 concentration was observed and where $[NO_2^-]_{amb}$ was <250 nM (two coastal ocean sites, the South China
584 Sea (SCS; Zhang et al., 2020) and Southern California Bight (SCB; Olson, 1981); one oligotrophic
585 ocean site, the subtropical South Atlantic (SSA; Fawcett et al. unpubl.); and two stations from the ETNP
586 ODZ, where oxygen concentrations ranged from 0 µM to 16.8 µM (Sun et al., 2017)). The robust
587 positive relationship of K_m to $[NO_2^-]_{amb}$ that emerges when these previous results are combined with
588 our Southern Ocean data ($R^2 = 0.68$, $p = 5.2 \times 10^{-5}$) strongly implicates $[NO_2^-]_{amb}$ as the dominant control
589 on the K_m of NO_2^- oxidation in the ocean, particularly at low $[NO_2^-]_{amb}$.
590
591 The production of NO_2^- from NH_4^+ oxidation has recently been hypothesized to be vulnerable to iron
592 limitation (Mdutyana, 2021) since AOB rely on iron-rich *cytochrome c* proteins (Arp et al., 2002;
593 Walker et al., 2010) and some AOA appear to have a low affinity for inorganic iron (Shafiee et al.,
594 2019). NOB also contain iron-rich enzymes, such as nitrite oxidoreductase, which is responsible for
595 converting NO_2^- to NO_3^- (Meincke et al., 1992; Spieck et al., 1998). While we have no iron data with
596 which to compare our kinetic parameters, dissolved iron concentrations ([DFe]) were measured at the
597 depth-profile stations (St 08 to St 11; Mdutyana, 2021). The revised NO_2^- oxidation rates at these
598 stations are weakly positively correlated with [DFe] ($R^2 = 0.35$, $p = 0.016$; Figure 5), indicating a
599 potential role for iron in controlling NO_2^- oxidation. Combined with the evidence that iron may also
600 constrain marine NH_4^+ oxidation (Shafiee et al., 2019), this observation implies that mixed-layer
601 nitrification in the Southern Ocean may be iron-limited. Since phytoplankton consumption of
602 regenerated NO_3^- yields no net removal of atmospheric CO_2 (Yool et al., 2007), an iron-related control
603 on mixed-layer nitrification would help to limit the extent to which this process can weaken the

https://doi.org/10.5194/bg-2021-280
Preprint. Discussion started: 29 October 2021

604 Southern Ocean's biological pump. It would also lead to enhanced competition between phytoplankton
605 and nitrifiers.

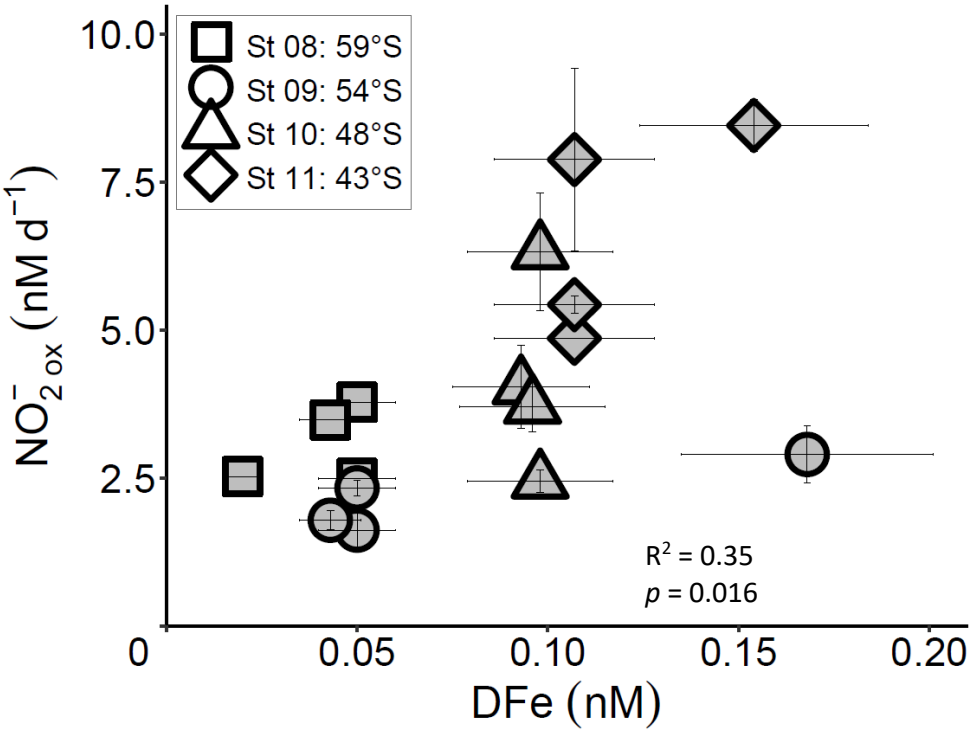

606

607 **Figure 5:** Euphotic zone (0-75 m) rates of NO_2^- oxidation measured at the depth-profile stations (St 08
608 to St 11) plotted against coincident dissolved iron concentrations (DFe). Error bars indicate the standard
609 error of replicate experiments/collections, each measured at least twice. Where errors bars are not
610 visible, they are smaller than the data markers.
611

612 4.3 The persistence of elevated NO_2^- concentrations throughout the Southern Ocean's mixed layer

613 While still limited, there is growing evidence that marine AOA have a very high affinity for NH_4^+ (more
614 correctly, ammonia (NH_3), the substrate for NH_4^+ oxidation; Mdutyana, 2021; Martens-Habbena et al.,
615 2009; Horak et al., 2013; Newell et al., 2013; Peng et al., 2016). Marine NOB also appear able to access
616 low concentrations of substrate, based on the few *in situ* studies conducted to-date, including this one
617 (Figure 4f; Olson, 1981; Sun et al., 2017; Zhang et al., 2020). This high substrate affinity is perhaps
618 unsurprising given that NO_2^- concentrations are generally near-zero throughout the oxygenated ocean,
619 rising modestly to values typically <500 nM at the PNM in (sub)tropical waters (Lomas and Lipschultz,
620 2006; Zakem et al., 2018) and <400 nM over the mixed layer in (sub)polar regions (Zakem et al., 2018).
621 The average surface NO_2^- concentration measured during Leg 1 of our cruise was 168 ± 48 nM (Figure
622 1a) and the average mixed-layer concentration for Leg 2 was 137 ± 57 nM (Figures 1b and 3a). Similar
623 concentrations have been observed previously across the Southern Ocean, including in other seasons

https://doi.org/10.5194/bg-2021-280
Preprint. Discussion started: 29 October 2021

(Cavagna et al., 2015; Fripiat et al., 2019; Mdutyana et al., 2020). Thus, while NO_2^- oxidation in Southern Ocean surface waters is characterized by a low K_m, the affinity of NOB for NO_2^- is apparently not high enough to completely remove the available NO_2^-.

The persistence of elevated NO_2^- concentrations in the mixed layer at high latitudes has been attributed to the inability of iron- and/or light-limited phytoplankton to fully consume NO_2^- transported to the surface with NO_3^- during deep mixing events (Zakem et al., 2018). However, subsurface NO_2^- concentrations in the Southern Ocean are typically below detection (Figure 1b and 3a; Olsen et al., 2016), so it is unclear how deep mixing could supply measurable NO_2^- to the euphotic zone.

A second possible source of elevated mixed-layer NO_2^- is efflux following partial NO_3^- reduction to NO_2^- by phytoplankton (Lomas and Lipschultz, 2006), which has been extensively documented in laboratory and field studies (see Collos, 1998 for a review). The release of NO_2^- by phytoplankton is hypothesized to result from light limitation of intracellular NO_2^- reduction (Vaccaro and Ryther, 1960; Kiefer et al., 1976), short-term increases in irradiance to which phytoplankton cannot adapt (Lomas and Lipschultz, 2006), iron limitation of NO_3^- assimilation (Milligan and Harrison, 2000), and/or release of phytoplankton from NO_3^- limitation following a period of starvation (Sciandra and Amara, 1994). While some of these mechanisms may be ongoing in the Southern Ocean, they all require the initial uptake of NO_3^- by phytoplankton. This process occurs in the winter mixed layer at rates that are too low to support NO_2^- efflux to the extent that it would allow NO_2^- to accumulate to concentrations of 100-300 nM (Figure S3; Philibert et al., 2015; Mdutyana et al., 2020) while simultaneously being removed by NO_2^- oxidation. Additionally, we observe a reasonable correlation between the NH_4^+ oxidation rates and ambient NO_2^- ($R^2 = 0.46$, $p = 0.0003$; Figure S4), which implies that NO_2^- derives mainly from NH_4^+ oxidation rather than phytoplankton efflux.

A third potential explanation for elevated mixed-layer NO_2^- is thus a decoupling of NH_4^+ and NO_2^- oxidation, which appears to be widespread in the environment (e.g., Ward and Zafiriou, 1988; Beman et al., 2013). In the oxygenated ocean, NH_4^+ oxidation has been considered the rate-limiting step in the nitrification pathway because NO_2^- seldom accumulates in the mixed layer (Kendall, 1998; Kowalchuk and Stephen, 2001; Walker et al., 2010; Vajrala et al., 2013). However, rate measurements from numerous ocean regions show contrasting results, with NO_2^- oxidation sometimes outpacing NH_4^+ oxidation (Peng et al., 2018; Dore and Karl, 1996; Bristow et al., 2015; Horrigan et al., 1990) while in other cases, NH_4^+ oxidation is dominant (Ward and Kilpatrick, 1991; Kalvelage et al., 2013; Clark et al., 2008). The limited data available from previous Southern Ocean investigations show no clear trend (Bianchi et al., 1997; Mdutyana et al., 2020). In the present study, mixed-layer $corrNO_2^-{}_{ox}$ rates are two- to seven-times lower than the coincidentally measured $corrNH_4^+{}_{ox}$ (Figures 3 and 6). Additionally, the maximum rates of NO_2^- oxidation (V_{max}) derived for the surface NOB community (~5 to 13 nM d^{-1};

https://doi.org/10.5194/bg-2021-280
Preprint. Discussion started: 29 October 2021

Figure 2) are on average half those determined at the same stations for NH_4^+ oxidation (14 to 23 nM d^{-1}; Mdutyana, 2021). At the time of our sampling, therefore, NO_2^- oxidation was rate-limiting for nitrification, which likely accounts for most of the NO_2^- accumulated in the Southern Ocean's winter mixed layer .

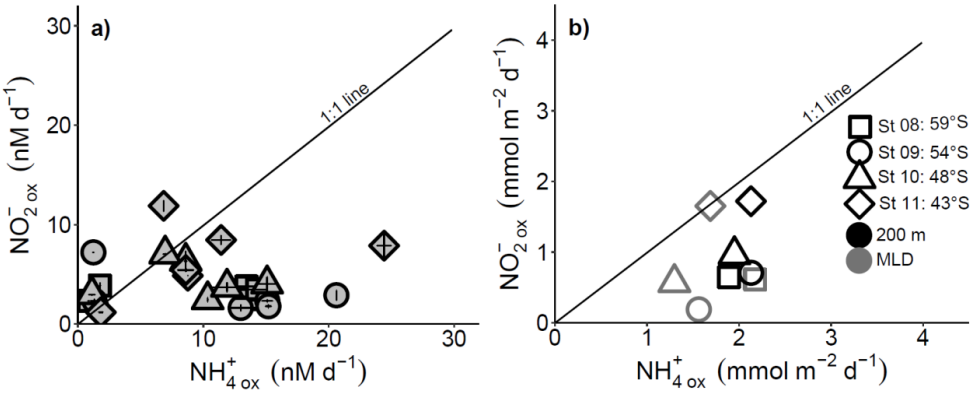

Figure 6: The relationship between the measured rates of NO_2^- and NH_4^+ oxidation for a) each experiment depth in the upper water column (0-500 m) and b) integrated over the mixed layer (grey symbols) and upper 200 m (black symbols). Error bars on panel a indicate the standard error of replicate experiments, each measured at least twice, while on panel b, error bars show the propagated error. Where errors bars are not visible, they are smaller than the data markers. The black diagonal line on both panels has a slope of 1, which is expected if the rates of NH_4^+ and NO_2^- oxidation are tightly coupled.

If a decoupling of NH_4^+ and NO_2^- oxidation is predominantly responsible for NO_2^- accumulation, an obvious question is why these rates are not balanced. Environmental factors like temperature, light, and/or pH may play a role (Ward, 2008; Heiss and Fulweiler, 2017), as may iron limitation and the different ecophysiologies of NH_4^+ and NO_2^- oxidizers. AOA have been shown to adapt more rapidly than NOB to a change in temperature (Schaefer and Hollibaugh, 2017); however, the seasonal SST variations within the various zones of the Southern Ocean are fairly small and the aforementioned study showing the differential thermal response of AOA and NOB was conducted at higher temperatures than those experienced in much of the Southern Ocean.

With regards to light, there is evidence from culture and field studies that NOB are more photosensitive than AOA and AOB (Bock, 1965; Olson, 1981b; Qin et al., 2014). Our data are consistent with this notion insofar as the V_{max} associated with NO_2^- oxidation in surface waters rises with increasing latitude (and thus decreasing light; Figure 4a) while the V_{max} derived for NH_4^+ oxidation remains largely unchanged across >30 degrees of latitude (Mdutyana, 2021). However, the ambient NO_2^- concentration in Southern Ocean surface waters rises near linearly with latitude (Figure S2a) while the NH_4^+ concentration resembles a step function, increasing from ~100 nM north of the SAF to ~700 nM

https://doi.org/10.5194/bg-2021-280
Preprint. Discussion started: 29 October 2021

690 south of the SAF, over a distance of roughly one degree of latitude (Figure S2b). The differing trends
691 in V_{max} may thus have more to do with substrate availability than photoinhibition.

692 Mixing, particularly deep winter overturning, might also contribute to a decoupling of NH_4^+ and NO_2^-
693 oxidation. In coastal waters, deep winter mixing has been shown to dilute the nitrifier community,
694 particularly NOB, leading to low rates of NO_2^- oxidation while NH_4^+ oxidation rates remain elevated,
695 ultimately causing NO_2^- accumulation in the upper layer (Haas et al., 2021). While a similar effect may
696 play a role in NO_2^- accumulation in the open Southern Ocean, it is unlikely that the entire NO_2^- reservoir
697 can be ascribed to this process. The rates of NH_4^+ oxidation are only slightly higher than NO_2^- oxidation
698 in the winter mixed layer (Figure 3) and the mixed-layer NH_4^+ concentrations are elevated (Figure 3f),
699 implying that NH_4^+ oxidizers are limited by something other than NH_4^+ substrate, preventing them from
700 catalysing higher rates of NO_2^- production (and thus NO_2^- accumulation).
701
702 A number of studies have shown the negative effect of decreasing pH on NH_4^+ oxidation in the ocean
703 (e.g., Huesemann et al., 2002; Beman et al., 2011; Kitidis et al., 2011), driven by a reduction in the
704 proportion of NH_3 relative to NH_4^+. By contrast, NO_2^- oxidation may increase as pH declines (Fulweiler
705 et al., 2011; Heiss and Fulweiler, 2017), although such a correlation has only been observed in one
706 coastal region. While a differential response of AOO and NOB to pH would decouple NH_4^+ and NO_2^-
707 oxidation, the resultant trend should be one of higher NO_2^- accumulation in the northern Southern Ocean
708 where surface pH is higher in winter and lower NO_2^- accumulation to the south where pH is lower (Key
709 et al., 2004; McNeil and Matear, 2008) – this is not the meridional pattern that we observe (Figure 1b).
710
711 Nitrite oxidoreductase (NXR), the enzyme possessed by NOB that is responsible for aerobic NO_2^-
712 oxidation to NO_3^-, is an iron-sulfur molybdoprotein (Sundermeyer-Klinger et al., 1984; Meincke et al.,
713 1992; Lücker et al., 2010). As such, NO_2^- oxidation has a significant iron requirement (Saito et al., 2020;
714 Bayer et al., 2021), intimated by the relationship we observe between $corrNO_2^-{}_{ox}$ and DFe (Figure 5).
715 Additionally, NO_2^- accumulation at the PNM in the California Current has been hypothesized to be
716 caused by iron limitation of NOB (Santoro et al., 2013). AOB also require iron, in particular for the
717 oxidation of hydroxylamine, which is catalyzed by the heme-rich hydroxylamine oxidoreductase
718 (HAO) complex (Arp et al., 2002; Walker et al., 2010). By contrast, AOA, the dominant marine NH_4^+
719 oxidizers, rely mainly on copper-containing proteins to mediate NH_4^+ oxidation (Amin et al., 2013;
720 Walker et al., 2010; Santoro et al., 2015). In the iron-limited Southern Ocean, it is thus possible that
721 iron scarcity more strongly limits NO_2^- than NH_4^+ oxidation. However, recent culture and proteomic
722 work suggests that some AOA may actually have a high iron requirement (Santoro et al., 2015; Carini
723 et al., 2018; Qin et al., 2018; Shafiee et al., 2019), and we have previously hypothesized an iron-related
724 control on NH_4^+ oxidation in the Southern Ocean (Mdutyana, 2021). Deeper investigation is thus

https://doi.org/10.5194/bg-2021-280
Preprint. Discussion started: 29 October 2021

725 required to characterize the role of iron in controlling the relative rates of NH_4^+ and NO_2^- oxidation, and
726 the implications for the complete nitrification pathway.
727
728 A further consideration is differences in the ecology of AOA and NOB. Marine NOB are an order of
729 magnitude less abundant than AOA (e.g., Füssel et al., 2012; Beman et al., 2013b; Pachiadaki et al.,
730 2017; Damashek et al., 2019; Kitzinger et al., 2020) and roughly three-times larger (Watson and
731 Waterbury, 1971; Könneke et al., 2005; Martens-Habbena et al., 2009; Pachiadaki et al., 2017). While
732 their affinity for NO_2^- appears to be high, the *in situ* K_m values derived to-date are not as low as those
733 reported for NH_4^+ oxidation (Horak et al., 2013; Peng et al., 2016; Xu et al., 2019; Zhang et al., 2020;
734 Mdutyana, 2021), which is perhaps to be expected given their larger size (Aksnes and Egge, 1991;
735 Litchman et al., 2007; Zakem et al., 2018). Additionally, the theoretical energy gain from NO_2^-
736 oxidation is lower than from NH_4^+ oxidation (Bock and Wagner, 2006), and it has been estimated that
737 NOB must consume three-times as much N as NH_4^+ oxidizers to produce the same amount of biomass
738 (Zakem et al., 2018). Nonetheless, a recent study from the Gulf of Mexico showed that NOB from the
739 phylum *Nitrospinae*, the dominant NO_2^- oxidizers in the ocean, grow five-times faster than AOA and
740 produce roughly four-times as much biomass despite their lower abundance, in part because they can
741 support up to half of their cellular N requirement using organic N compounds such as urea (Kitzinger
742 et al., 2020). This study was conducted in hypoxic shelf waters, however, such that the applicability of
743 its findings to the Southern Ocean is unclear. Nevertheless, it seems likely that the very different life
744 strategies of NH_4^+ and NO_2^- oxidizers play a role in decoupling the steps of nitrification in the Southern
745 Ocean.
746
747 Resource limitation theory posits that nitrifiers require a subsistence concentration of substrate (R*) to
748 maintain their population, and that those with the lowest R* will outcompete all other organisms limited
749 by the same resource, provided their V_{max} is greater than their loss rate due to grazing and/or viral lysis
750 (Zakem et al., 2018). Because NOB are considerably larger than AOA (Watson and Waterbury, 1971;
751 Könneke et al., 2005; Martens-Habbena et al., 2009; Pachiadaki et al., 2017), they will have a higher
752 R* than AOA even before grazing pressure is factored in. Their large size also means that NOB are
753 more likely to be grazed than AOA, which will further increase their R*, as will the fact that their
754 maximum growth rates are slow and thus vulnerable to being outpaced by their loss rate. Taken together,
755 these factors will increase R*, potentially resulting in the accumulation of NO_2^- in the water column,
756 and may help to explain why the K_m for NO_2^- oxidation, in the Southern Ocean and elsewhere, is
757 considerably higher than that derived for NH_4^+ oxidation. Additionally, the fact that NOB will be
758 preferentially grazed over AOA may contribute to NO_2^- oxidation being rate-limiting for nitrification.
759
760 That NO_2^- oxidation was rate-limiting at the time of our sampling does not necessarily explain the
761 accumulation of NO_2^- in the Southern Ocean mixed layer year-round. Neither NH_4^+ nor NO_2^- oxidation

https://doi.org/10.5194/bg-2021-280
Preprint. Discussion started: 29 October 2021

occur at elevated rates in summer or autumn (Bianchi et al., 1997; Mdutyana et al., 2020), yet the elevated NO_2^- concentrations persist during these seasons (Cavagna et al., 2015; Fripiat et al., 2019; Mdutyana et al., 2020). To fit a Michaelis-Menten curve to our experimental data required amending the classical equation (equation 2) to allow for a positive x-intercept (i.e., a non-zero S value at which V was still zero, denoted as the C parameter in equation 3) (Archontoulis and Miguez, 2014). Additionally, at most stations, the NO_2^- oxidation rates did not increase substantially following the initial two or three substrate amendments (i.e., in Figure 2, the slope of the relationship between V and S is less steep for the initial two to three values of S than at higher values). Practically, our findings suggest that Southern Ocean NOB require a minimum (i.e., "threshold") NO_2^- concentration below which, NO_2^- becomes severely limiting. Coupled with weak NO_2^- drawdown by iron- and/or light-limited phytoplankton during their incomplete consumption of the NO_3^-+NO_2^- pool, a threshold substrate requirement of NOB can explain the year-round persistence of non-zero mixed-layer NO_2^- since it implies that there is no mechanism by which NO_2^- can be completely exhausted.

We hypothesize that the NO_2^- concentration threshold is indicative of an undersaturation by substrate NO_2^- of NXR, which is a membrane-bound enzyme (Lücker et al., 2010; Sundermeyer-Klinger et al., 1984) that occurs in two forms: 1) with the substrate-binding subunit (NxrA) orientated outwards into the periplasmic space, as in *Nitrospira* and *Nitrospina* (Spieck et al., 1998; Lücker et al., 2010; 2013; Koch et al., 2015; Daims et al., 2016) and 2) with NxrA orientated inward towards the cytoplasm, as in *Nitrococcus* and *Nitrobacter* (Spieck et al., 1996; Starkenburg et al., 2006; Sorokin et al., 2012). The dominant genera of NOB in the ocean are *Nitrospina* and *Nitrospira* (Beman et al., 2013; Füssel et al., 2012), with a recent metaproteomic study identifying *Nitrospina* NXR as the most abundant microbial protein in the mesopelagic zone of the Central Tropical Pacific (Saito et al., 2020). If *Nitrospina* (and/or *Nitrospira*) is similarly abundant across the Southern Ocean, as has been intimated for the Pacific Subantarctic (Raes et al., 2020), the fact that its NXR is contained within the periplasmic space suggests that substrate undersaturation is possible. This is in contrast to NOB with a cytoplasmic NXR that must first transport NO_2^- across the cell membrane and into the cytoplasm where it can accumulate to saturating concentrations before being oxidized (Daims et al., 2016). These NOB (i.e., *Nitrococcus* and *Nitrobacter*) have a lower NO_2^- affinity than those with a periplasmic NXR (Schramm et al., 1999; Nowka et al., 2015), with the latter group thus better suited to regions of low NO_2^-. Nonetheless, our data suggest the NXR in the Southern Ocean, probably associated with *Nitrospina* and *Nitrospira* (Raes et al., 2020), is substrate-limited, resulting in a perennially elevated concentration of NO_2^- in the mixed layer.

Nitrospina and *Nitrospira* are ubiquitous in the ocean (Beman et al., 2013; Füssel et al., 2012), which raises the question of why a similar NO_2^- concentration threshold has not been reported from other regions. This may partly be due to the very limited number of NO_2^- oxidation kinetics experiments that

https://doi.org/10.5194/bg-2021-280
Preprint. Discussion started: 29 October 2021

have been conducted in the open ocean and/or to the fact that a classic Michaelis-Menten function is usually imposed upon kinetics data, with V assumed to increase as soon as S > 0. Additionally, depending on the maximum substrate concentration added during kinetics experiments, it can be difficult to discern a possible threshold NO_2^- concentration by simply examining the resultant plots. Inspection of published Michaelis-Menten curves reveals the possibility of a non-zero C value in some cases, including in the ETNP ODZ (Sun et al., 2021) and associated with the PNM in the South China Sea (Zhang et al., 2020). However, there are other published curves that clearly do intercept the origin in V versus S space (Olson, 1981a; Sun et al., 2017), which may indicate a different NOB community (e.g., dominated by *Nitrococcus*). Alternately, environmental factors unique to the Southern Ocean, such as light, temperature, and/or iron availability, may be instrumental in setting the NO_2^- threshold and associated elevated mixed-layer NO_2^- concentrations that we observe. Indeed, iron limitation of NXR could be implicit in its tendency towards NO_2^- undersaturation. Using NXR concentrations, estimates of NXR specific activity, and direct measurements of *in situ* NO_2^- oxidation rates, Saito et al., (2020) recently deduced that *Nitrospina* NXR is undersaturated with NO_2^- in the iron-limited tropical Pacific. This finding is consistent with the mechanism we invoke to explain the apparent NO_2^- concentration threshold in the Southern Ocean, as well as with the existence of such a threshold indicating *Nitrospina* (and/or *Nitrospira*) dominance of the *in situ* NOB community.

5. Concluding remarks

In this study, we present the first NO_2^- oxidation kinetic constants for the Southern Ocean, deriving from surface experiments conducted during winter 2017. All the experiments were well-described by the Michaelis-Menten equation, provided that a location parameter, C, was included in the model. V_{max} ranged from 5.2 ± 0.1 to 13 ± 0.4 nM d^{-1} and K_m ranged from 134 ± 8 to 403 ± 24 nM, with the latter parameter showing a strong positive relationship with the ambient NO_2^- concentration. We interpret the positive values of C (range of 115 ± 2.3 to 245 ± 18 nM) to indicate an ambient NO_2^- concentration threshold below which NOB are impeded. Additionally, we hypothesize that this threshold indicates substrate limitation of NXR, possibly exacerbated by the low ambient iron concentrations characteristic of the upper Southern Ocean. From depth-profile measurements, we deduce that the rate-limiting step for mixed-layer nitrification in the winter is NO_2^- oxidation. Despite this, NO_3^- production from NO_2^- oxidation accounted for 63-237% of the NO_3^- consumed by phytoplankton, consistent with previous wintertime observations from the Atlantic Southern Ocean (Mdutyana et al., 2020).

NO_2^- oxidation, as the ultimate step that connects reduced N to its most oxidized form (NO_3^-), is important throughout the water column, but particularly in the upper layer where the supply of reduced N is highest. The production of NO_3^- within the mixed layer from *in situ* nitrification can complicate the application of the new production paradigm as a framework for estimating export production (Yool et al., 2007; Mdutyana et al., 2020), which advocates for additional measurements of this pathway over

https://doi.org/10.5194/bg-2021-280
Preprint. Discussion started: 29 October 2021

the upper ~200 m. Additionally, it is becoming increasingly clear that we lack a mechanistic understanding of the controls on nitrification (both NH_4^+ and NO_2^- oxidation), which renders it challenging to model both its magnitude and distribution, as well as to assess how these may change in future. In particular, further study of the role of iron in controlling nitrification is required, particularly in the Southern Ocean where the mixed layer's biological N cycle is dominated by nitrification in winter (Smart et al., 2015; Mdutyana et al., 2020) and surface-layer iron is very low throughout the year (Tagliabue et al., 2012).

Acknowledgements

We thank Captain Knowledge Bengu and the crew of the R/V *S.A. Agulhas II* and Chief Scientist M. Vichi for professional support during the cruise, as well as the Marine Biogeochemistry Lab team at the University of Cape Town (UCT), C. Karriem for extensive administrative support, and I. Newton and J. Luyt at the UCT Stable Light Isotope Laboratory for filter analyses. The nitrification measurements were made possible through the Princeton University Visiting Student Research Collaborator program – we are especially grateful to S. Oleynik in the Department of Geosciences for his expert assistance during the first author's visit. This work was supported by the South African National Research Foundation through Antarctic Programme grants to S.E.F. (110735, 129232), and S.J.T. (93076), and postgraduate scholarships to M.M. (112380), T.M. (114673 and 130826) and J.M.B. (110732); by UCT through a Harry Crossley Foundation Research Fellowship to M.M., postgraduate scholarship to T.M., Vice-Chancellor (VC) Research Scholarships to J.M.B., a VC Future Leaders 2030 award to S.E.F., and a Research Committee Equipment grant to S.E.F.; by the African Academy of Sciences/Royal Society through a FLAIR Fellowship to S.E.F; and by US National Science Foundation grants to B.B.W. The authors also acknowledge the South African Department of Science and Innovation's Biogeochemistry Research Infrastructure Platform.

https://doi.org/10.5194/bg-2021-280
Preprint. Discussion started: 29 October 2021

References

Aksnes, D. L., and J. K. Egge. 1991. "A_theoretical_model_for_nutrient_uptake_in_phytoplankton." *Marine Ecology Progress Series*.

Amin, Shady A., James W. Moffett, Willm Martens-Habbena, Jeremy E. Jacquot, Yang Han, Allan Devol, Anitra E. Ingalls, David A. Stahl, and E. Virginia Armbrust. 2013. "Copper Requirements of the Ammonia-Oxidizing Archaeon Nitrosopumilus Maritimus SCM1 and Implications for Nitrification in the Marine Environment." *Limnology and Oceanography* 58 (6): 2037–45. https://doi.org/10.4319/lo.2013.58.6.2037.

Archontoulis, Sotirios V., and Fernando E. Miguez. 2014. "Nonlinear Regression Models and Applications in Agricultural Research." *Agronomy Journal* 107 (2): 786–98. https://doi.org/10.2134/agronj2012.0506.

Arp, Daniel J., Luis A. Sayavedra-Soto, and Norman G. Hommes. 2002. "Molecular Biology and Biochemistry of Ammonia Oxidation by Nitrosomonas Europaea." *Archives of Microbiology* 178 (4): 250–55. https://doi.org/10.1007/s00203-002-0452-0.

Baer, S. E., T. L. Connelly, R. E. Sipler, P. L. Yager, and D. A. Bronk. 2014. "Effect of Temperature on Rates of Ammonium Uptake and Nitrification in the Western Coastal Arctic during Winter, Spring, and Summer." *Global Biogeochemical Cycles* 28: 1455–66. https://doi.org/10.1111/1462-2920.13280.

Bayer, Barbara, Mak A. Saito, Matthew R. McIlvin, Sebastian Lücker, Dawn M. Moran, Thomas S. Lankiewicz, Christopher L. Dupont, and Alyson E. Santoro. 2021. "Metabolic Versatility of the Nitrite-Oxidizing Bacterium Nitrospira Marina and Its Proteomic Response to Oxygen-Limited Conditions." *ISME Journal* 15 (4): 1025–39. https://doi.org/10.1038/s41396-020-00828-3.

Belkin, Igor M., and Arnold L. Gordon. 1996. "Southern Ocean Fronts from the Greenwich Meridian to Tasmania." *Journal of Geophysical Research C: Oceans*. https://doi.org/10.1029/95JC02750.

Beman, J. Michael, Cheryl Emiliane Chow, Andrew L. King, Yuanyuan Feng, Jed A. Fuhrman, Andreas Andersson, Nicholas R. Bates, Brian N. Popp, and David A. Hutchins. 2011. "Global Declines in Oceanic Nitrification Rates as a Consequence of Ocean Acidification." *Proceedings of the National Academy of Sciences of the United States of America* 108 (1): 208–13. https://doi.org/10.1073/pnas.1011053108.

Beman, J. Michael, Joy Leilei Shih, and Brian N. Popp. 2013. "Nitrite Oxidation in the Upper Water Column and Oxygen Minimum Zone of the Eastern Tropical North Pacific Ocean." *ISME Journal* 7 (11): 2192–2205. https://doi.org/10.1038/ismej.2013.96.

Beman, J. Michael, Brian N. Popp, and Christopher A. Francis. 2008. "Molecular and Biogeochemical Evidence for Ammonia Oxidation by Marine Crenarchaeota in the Gulf of California." *ISME Journal* 2 (4): 429–41. https://doi.org/10.1038/ismej.2007.118.

Bianchi, Micheline, F. Feliatra, Paul Tréguer, Marie Anne Vincendeau, and Jean Morvan. 1997. "Nitrification Rates, Ammonium and Nitrate Distribution in Upper Layers of the Water Column and in Sediments of the Indian Sector of the Southern Ocean." *Deep-Sea Research Part II: Topical Studies in Oceanography* 44 (5): 1017–32. https://doi.org/10.1016/S0967-0645(96)00109-9.

Birch, Colin P.D. 1999. "A New Generalized Logistic Sigmoid Growth Equation Compared with the Richards Growth Equation." *Annals of Botany* 83 (6): 713–23. https://doi.org/10.1006/anbo.1999.0877.

Blackburne, Richard, Vel M Vadivelu, and Zhiguo Yuan. 2007. "Kinetic Characterisation of an Enriched Nitrospira Culture with Comparison to Nitrobacter" 41: 3033–42. https://doi.org/10.1016/j.watres.2007.01.043.

https://doi.org/10.5194/bg-2021-280
Preprint. Discussion started: 29 October 2021

Bock, Eberhard. 1965. "Vergleichende Untersuchungen Über Die Wirkung Sichtbaren Lichtes Auf Nitrosomonas Europaea Und Nitrobacter Winogradskyi." *Archiv Für Mikrobiologie*. https://doi.org/10.1007/BF00406848.

Bock, Eberhard, and Michael Wagner. 2006. *Ox i Dat i on of Inorgan i c N i Trogen Compound s a s an Energy Source*.

Bristow, Laura A., Neha Sarode, John Cartee, Alejandro Caro-Quintero, Bo Thamdrup, and Frank J. Stewart. 2015. "Biogeochemical and Metagenomic Analysis of Nitrite Accumulation in the Gulf of Mexico Hypoxic Zone." *Limnology and Oceanography* 60 (5): 1733–50. https://doi.org/10.1002/lno.10130.

Caranto, Jonathan D., and Kyle M. Lancaster. 2017. "Nitric Oxide Is an Obligate Bacterial Nitrification Intermediate Produced by Hydroxylamine Oxidoreductase." *Proceedings of the National Academy of Sciences of the United States of America* 114 (31): 8217–22. https://doi.org/10.1073/pnas.1704504114.

Carini, Paul, Christopher L. Dupont, and Alyson E. Santoro. 2018. "Patterns of Thaumarchaeal Gene Expression in Culture and Diverse Marine Environments." *Environmental Microbiology* 20 (6): 2112–24. https://doi.org/10.1111/1462-2920.14107.

Carvalho, Filipa, Josh Kohut, Matthew J. Oliver, and Oscar Schofield. 2017. "Defining the Ecologically Relevant Mixed-Layer Depth for Antarctica's Coastal Seas." *Geophysical Research Letters*. https://doi.org/10.1002/2016GL071205.

Cavagna, A. J., F. Fripiat, M. Elskens, P. Mangion, L. Chirurgien, I. Closset, M. Lasbleiz, et al. 2015. "Production Regime and Associated N Cycling in the Vicinity of Kerguelen Island, Southern Ocean." *Biogeosciences* 12 (21): 6515–28. https://doi.org/10.5194/bg-12-6515-2015.

Clark, Darren R, Andrew P Rees, Ian Joint, Source Limnology, No Jan, Darren R Clark, Andrew P Rees, and Ian Joint. 2008. "Ammonium Regeneration and Nitrification Rates in the Oligo Trophic Atlantic Ocean : Implications for New Production Estimates." *Limnology and Oceanography* 53 (1): 52–62.

Collos, Yves. 1998. "Nitrate Uptake, Nitrite Release and Uptake, and New Production Estimates." *Marine Ecology Progress Series* 171: 293–301. https://doi.org/10.3354/meps171293.

Daims, Holger, Sebastian Lücker, and Michael Wagner. 2016. "A New Perspective on Microbes Formerly Known as Nitrite-Oxidizing Bacteria." *Trends in Microbiology* 24 (9): 699–712. https://doi.org/10.1016/j.tim.2016.05.004.

Damashek, Julian, Bradley B. Tolar, Qian Liu, Aimee O. Okotie-Oyekan, Natalie J. Wallsgrove, Brian N. Popp, and James T. Hollibaugh. 2019. "Microbial Oxidation of Nitrogen Supplied as Selected Organic Nitrogen Compounds in the South Atlantic Bight." *Limnology and Oceanography* 64 (3): 982–95. https://doi.org/10.1002/lno.11089.

DeVries, Tim, Mark Holzer, and Francois Primeau. 2017. "Recent Increase in Oceanic Carbon Uptake Driven by Weaker Upper-Ocean Overturning." *Nature* 542 (7640): 215–18. https://doi.org/10.1038/nature21068.

Diaz, Frédéric, and Patrick Raimbault. 2000. "Nitrogen Regeneration and Dissolved Organic Nitrogen Release during Spring in a NW Mediterranean Coastal Zone (Gulf of Lions): Implications for the Estimation of New Production." *Marine Ecology Progress Series* 197: 51–65. https://doi.org/10.3354/meps197051.

DiFiore, Peter J., Daniel M. Sigman, and Robert B. Dunbar. 2009. "Upper Ocean Nitrogen Fluxes in the Polar Antarctic Zone: Constraints from the Nitrogen and Oxygen Isotopes of Nitrate." *Geochemistry, Geophysics, Geosystems* 10 (11). https://doi.org/10.1029/2009GC002468.

Dore, John E, and David A I Karl. 1996. "Nitrification in the Euphotic Zone as a Source for Nitrite ,

955 Nitrate , and Nitrous Oxide at Station ALOHA" 41: 1619–28.

956 Dugdale, R. C., and J. J. Goering. 1967. "Uptake of New and Regenerated Forms of Nitrogen in
957 Primary Productivity." *Limnology and Oceanography* 12 (2): 196–206.
958 https://doi.org/10.4319/lo.1967.12.2.0196.

959 Dugdale, R C, and F P Wilkerson. 1986. "The Use of N-15 To Measure Nitrogen Uptake in Eutrophic
960 Oceans - Experimental Considerations." *Limnology and Oceanography* 31 (4): 673–89.

961 Eppley, Richard W., and Bruce J. Peterson. 1979. "Particulate Organic Matter Flux and Planktonic
962 New Production in the Deep Ocean." *Nature* 282 (5740): 677–80.
963 https://doi.org/10.1038/282677a0.

964 Fripiat, François, Anja S. Studer, Gerald H. Haug, Sergey Oleynik, Alfredo Martínez-García, Sandi
965 M. Smart, Florian Rubach, Daniel M. Sigman, Sarah E. Fawcett, and Preston C. Kemeny. 2019.
966 "The Isotope Effect of Nitrate Assimilation in the Antarctic Zone: Improved Estimates and
967 Paleoceanographic Implications." *Geochimica et Cosmochimica Acta* 247: 261–79.
968 https://doi.org/10.1016/j.gca.2018.12.003.

969 Fulweiler, Robinson W., Hollie E. Emery, Elise M. Heiss, and Veronica M. Berounsky. 2011.
970 "Assessing the Role of PH in Determining Water Column Nitrification Rates in a Coastal
971 System." *Estuaries and Coasts* 34 (6): 1095–1102. https://doi.org/10.1007/s12237-011-9432-4.

972 Füssel, Jessika, Phyllis Lam, Gaute Lavik, Marlene M. Jensen, Moritz Holtappels, Marcel Günter, and
973 Marcel M.M. Kuypers. 2012. "Nitrite Oxidation in the Namibian Oxygen Minimum Zone."
974 *ISME Journal* 6 (6): 1200–1209. https://doi.org/10.1038/ismej.2011.178.

975 Glibert, Patricia M., Mark R. Dennett, and Joel C. Goldman. 1985. "Inorganic Carbon Uptake by
976 Phytoplankton in Vineyard Sound, Massachusetts. II. Comparative Primary Productivity and
977 Nutritional Status of Winter and Summer Assemblages." *Journal of Experimental Marine*
978 *Biology and Ecology* 86 (2). https://doi.org/10.1016/0022-0981(85)90025-5.

979 Glibert, Patricia M., Fredric Lipschultz, James J. Mccarthy, and Mark a. Altabet. 1982. "Isotope
980 Dilution Models of Uptake and Remineralization of Ammonium By Marine Plankton."
981 *Limnology and Oceanography* 27 (4): 639–50. https://doi.org/10.4319/lo.1982.27.4.0639.

982 Grasshoff K, Ehrhardt M, and, Kremling K. 1983. *Methods of Seawater Analysis*. Verlag Chemie,
983 New York.

984 Gruber, Nicolas, Dominic Clement, Brendan R. Carter, Richard A. Feely, Steven van Heuven, Mario
985 Hoppema, Masao Ishii, et al. 2019. "The Oceanic Sink for Anthropogenic CO 2 from 1994 to
986 2007." *Science* 363 (6432): 1193–99. https://doi.org/10.1126/science.aau5153.

987 Haas, Sebastian, Brent M. Robicheau, Subhadeep Rakshit, Jennifer Tolman, Christopher K. Algar,
988 Julie LaRoche, and Douglas W.R. Wallace. 2021. "Physical Mixing in Coastal Waters Controls
989 and Decouples Nitrification via Biomass Dilution." *Proceedings of the National Academy of*
990 *Sciences of the United States of America* 118 (18). https://doi.org/10.1073/pnas.2004877118.

991 Hauck, J., C. Völker, D. A. Wolf-Gladrow, C. Laufkötter, M. Vogt, O. Aumont, L. Bopp, et al. 2015.
992 "On the Southern Ocean CO2 Uptake and the Role of the Biological Carbon Pump in the 21st
993 Century." *Global Biogeochemical Cycles* 29 (9): 1451–70.
994 https://doi.org/10.1002/2015GB005140.

995 Heiss, Elise M., and Robinson W. Fulweiler. 2017. "Erratum to 'Coastal Water Column Ammonium
996 and Nitrite Oxidation Are Decoupled in Summer' (Estuarine, Coastal and Shelf Science (2016)
997 178 (110–119) (S0272771417301981) (10.1016/j.Ecss.2017.02.023))." *Estuarine, Coastal and*
998 *Shelf Science* 193: 37–45. https://doi.org/10.1016/j.ecss.2016.12.026.

999 Holmes, R M, A Aminot, R Kerouel, B A Hooker, and B J Peterson. 1999. "A Simple and Precise
1000 Method for Measuring Ammonium in Marine and Freshwater Ecosystems." *Canadian Journal*

of Fisheries and Aquatic Sciences. https://doi.org/10.1139/cjfas-56-10-1801.

Horak, Rachel E.A., Wei Qin, Andy J. Schauer, E. Virginia Armbrust, Anitra E. Ingalls, James W. Moffett, David A. Stahl, and Allan H. Devol. 2013. "Ammonia Oxidation Kinetics and Temperature Sensitivity of a Natural Marine Community Dominated by Archaea." *ISME Journal* 7 (10): 2023–33. https://doi.org/10.1038/ismej.2013.75.

Horrigan, S. G., J. P. Montoya, J. L. Nevins, J. J. McCarthy, H. Ducklow, R. Goericke, and T. Malone. 1990. "Nitrogenous Nutrient Transformations in the Spring and Fall in the Chesapeake Bay." *Estuarine, Coastal and Shelf Science* 30 (4). https://doi.org/10.1016/0272-7714(90)90004-B.

Huesemann, Michael H., Ann D. Skillman, and Eric A. Crecelius. 2002. "The Inhibition of Marine Nitrification by Ocean Disposal of Carbon Dioxide." *Marine Pollution Bulletin* 44 (2): 142–48. https://doi.org/10.1016/S0025-326X(01)00194-1.

Jacob, Juliane, Boris Nowka, Véronique Merten, Tina Sanders, Eva Spieck, and Kirstin Dähnke. 2017. "Oxidation Kinetics and Inverse Isotope Effect of Marine Nitrite-Oxidizing Isolates." *Aquatic Microbial Ecology* 80 (3): 289–300. https://doi.org/10.3354/ame01859.

Jong, Ehlke de, Marcello Vichi, Carolin Birgitta Mehlmann, Clare Eayrs, Wade De Kock, Marcel Moldenhauer, and Riesna Reuben Audh. 2018. "Sea Ice Conditions within the Antarctic Marginal Ice Zone in Winter 2017, Onboard the SA Agulhas II." *Pangaea*, 2018. https://doi.org/10.1594/PANGAEA.885211.

Kalvelage, Tim, Gaute Lavik, Phyllis Lam, Sergio Contreras, Lionel Arteaga, Carolin R. Löscher, Andreas Oschlies, Aurélien Paulmier, Lothar Stramma, and Marcel M.M. Kuypers. 2013. "Nitrogen Cycling Driven by Organic Matter Export in the South Pacific Oxygen Minimum Zone." *Nature Geoscience* 6 (3): 228–34. https://doi.org/10.1038/ngeo1739.

Kendall, Carol. 1998. "USGS -- Isotope Tracers -- Resources: Isotope Tracers in Catchment Hydrology -- Chapter 16." *Isotope Tracers in Catchment Hydrology Elsevier Science B.V.*

Key, R. M., A. Kozyr, C. L. Sabine, K. Lee, R. Wanninkhof, J. L. Bullister, R. A. Feely, F. J. Millero, C. Mordy, and T. H. Peng. 2004. "A Global Ocean Carbon Climatology: Results from Global Data Analysis Project (GLODAP)." *Global Biogeochemical Cycles* 18 (4): 1–23. https://doi.org/10.1029/2004GB002247.

Khatiwala, S., F. Primeau, and T. Hall. 2009. "Reconstruction of the History of Anthropogenic CO2 Concentrations in the Ocean." *Nature* 462 (7271): 346–49. https://doi.org/10.1038/nature08526.

Kiefer, D. A., R. J. Olson, and O. Holm-Hansen. 1976. "Another Look at the Nitrite and Chlorophyll Maxima in the Central North Pacific." *Deep-Sea Research and Oceanographic Abstracts* 23 (12). https://doi.org/10.1016/0011-7471(76)90895-0.

Kitidis, Vassilis, Bonnie Laverock, Louise C. McNeill, Amanda Beesley, Denise Cummings, Karen Tait, Mark A. Osborn, and Stephen Widdicombe. 2011. "Impact of Ocean Acidification on Benthic and Water Column Ammonia Oxidation." *Geophysical Research Letters* 38 (21): 2–6. https://doi.org/10.1029/2011GL049095.

Kits, K. Dimitri, Christopher J. Sedlacek, Elena V. Lebedeva, Ping Han, Alexandr Bulaev, Petra Pjevac, Anne Daebeler, et al. 2017. "Kinetic Analysis of a Complete Nitrifier Reveals an Oligotrophic Lifestyle." *Nature* 549 (7671): 269–72. https://doi.org/10.1038/nature23679.

Kitzinger, Katharina, Hannah K. Marchant, Laura A. Bristow, Craig W. Herbold, Cory C. Padilla, Abiel T. Kidane, Sten Littmann, et al. 2020. "Single Cell Analyses Reveal Contrasting Life Strategies of the Two Main Nitrifiers in the Ocean." *Nature Communications* 11 (1). https://doi.org/10.1038/s41467-020-14542-3.

Koch, Hanna, Sebastian Lücker, Mads Albertsen, Katharina Kitzinger, Craig Herbold, Eva Spieck,

https://doi.org/10.5194/bg-2021-280
Preprint. Discussion started: 29 October 2021

1047 Per Halkjaer Nielsen, Michael Wagner, and Holger Daims. 2015. "Expanded Metabolic
1048 Versatility of Ubiquitous Nitrite-Oxidizing Bacteria from the Genus Nitrospira." *Proceedings of*
1049 *the National Academy of Sciences of the United States of America* 112 (36): 11371–76.
1050 https://doi.org/10.1073/pnas.1506533112.

1051 Kowalchuk, G. A., and J. R. Stephen. 2001. "Ammonia-Oxidizing Bacteria: A Model for Molecular
1052 Microbial Ecology." *Annual Review of Microbiology* 55: 485–529.
1053 https://doi.org/10.1146/annurev.micro.55.1.485.

1054 Kozlowski, Jessica A., Michaela Stieglmeier, Christa Schleper, Martin G. Klotz, and Lisa Y. Stein.
1055 2016. "Pathways and Key Intermediates Required for Obligate Aerobic Ammonia-Dependent
1056 Chemolithotrophy in Bacteria and Thaumarchaeota." *ISME Journal* 10 (8): 1836–45.
1057 https://doi.org/10.1038/ismej.2016.2.

1058 Litchman, Elena, Christopher A. Klausmeier, Oscar M. Schofield, and Paul G. Falkowski. 2007. "The
1059 Role of Functional Traits and Trade-Offs in Structuring Phytoplankton Communities: Scaling
1060 from Cellular to Ecosystem Level." *Ecology Letters* 10 (12): 1170–81.
1061 https://doi.org/10.1111/j.1461-0248.2007.01117.x.

1062 Lomas, Michael W., and Fredric Lipschultz. 2006. "Forming the Primary Nitrite Maximum: Nitrifiers
1063 or Phytoplankton?" *Limnology and Oceanography* 51 (5): 2453–67.
1064 https://doi.org/10.4319/lo.2006.51.5.2453.

1065 Lücker, Sebastian, Boris Nowka, Thomas Rattei, Eva Spieck, and Holger Daims. 2013. "The Genome
1066 of Nitrospina Gracilis Illuminates the Metabolism and Evolution of the Major Marine Nitrite
1067 Oxidizer." *Frontiers in Microbiology* 4 (FEB). https://doi.org/10.3389/fmicb.2013.00027.

1068 Lücker, Sebastian, Michael Wagner, Frank Maixner, Eric Pelletier, Hanna Koch, Benoit Vacherie,
1069 Thomas Rattei, et al. 2010. "A Nitrospira Metagenome Illuminates the Physiology and
1070 Evolution of Globally Important Nitrite-Oxidizing Bacteria." *Proceedings of the National*
1071 *Academy of Sciences of the United States of America* 107 (30): 13479–84.
1072 https://doi.org/10.1073/pnas.1003860107.

1073 Martens-Habbena, Willm, Paul M. Berube, Hidetoshi Urakawa, José R. De La Torre, and David A.
1074 Stahl. 2009. "Ammonia Oxidation Kinetics Determine Niche Separation of Nitrifying Archaea
1075 and Bacteria." *Nature* 461 (7266): 976–79. https://doi.org/10.1038/nature08465.

1076 McIlvin, Matthew R., and Karen L. Casciotti. 2011. "Technical Updates to the Bacterial Method for
1077 Nitrate Isotopic Analyses." *Analytical Chemistry* 83 (5): 1850–56.
1078 https://doi.org/10.1021/ac1028984.

1079 McNeil, Ben I., and Richard J. Matear. 2008. "Southern Ocean Acidification: A Tipping Point at 450-
1080 Ppm Atmospheric CO2." *Proceedings of the National Academy of Sciences of the United States*
1081 *of America* 105 (48): 18860–64. https://doi.org/10.1073/pnas.0806318105.

1082 Mdutyana, Mhlangabezi. 2021. "Mixed Layer Nitrogen Cycling in the Southern Ocean: Seasonality,
1083 Kinetics, and Biogeochemical Implications A Thesis Presented for the Degree Of." *University of*
1084 *Cape Town, PhD Thesis*, no. June.

1085 Mdutyana, Mhlangabezi, Sandy J. Thomalla, R. Philibert, Bess B. Ward, and Sarah E. Fawcett. 2020.
1086 "The Seasonal Cycle of Nitrogen Uptake and Nitrification in the Atlantic Sector of the Southern
1087 Ocean." *Global Biogeochemical Cycles*, no. 3: 1–29. https://doi.org/10.1029/2019GB006363.

1088 Meincke, Michael, Eberhard Bock, Dieter Kastrau, and Peter M.H. Kroneck. 1992. "Nitrite
1089 Oxidoreductase from Nitrobacter Hamburgensis: Redox Centers and Their Catalytic Role."
1090 *Archives of Microbiology* 158 (2): 127–31. https://doi.org/10.1007/BF00245215.

1091 Milligan, Allen J., and Paul J. Harrison. 2000. "Effects of Non-Steady-State Iron Limitation on
1092 Nitrogen Assimilatory Enzymes in the Marine Diatom Thalassiosira Weissflogii

(Bacillariophyceae).” *Journal of Phycology* 36 (1): 78–86. https://doi.org/10.1046/j.1529-8817.2000.99013.x.

Monod, Jacques. 1942. “Recherches Sur La Croissance Des Cultures Bacteriennes.” *Hermann and Cie, Paris.*

Moore, C. M., M. M. Mills, K. R. Arrigo, I. Berman-Frank, L. Bopp, P. W. Boyd, E. D. Galbraith, et al. 2013. “Processes and Patterns of Oceanic Nutrient Limitation.” *Nature Geoscience* 6 (9): 701–10. https://doi.org/10.1038/ngeo1765.

Mulholland, Margaret R., and Peter W. Bernhardt. 2005. “The Effect of Growth Rate, Phosphorus Concentration, and Temperature on N2 Fixation, Carbon Fixation, and Nitrogen Release in Continuous Cultures of Trichodesmium IMS101.” *Limnology and Oceanography* 50 (3): 839–49. https://doi.org/10.4319/lo.2005.50.3.0839.

Newell, Silvia E., Andrew R. Babbin, Amal Jayakumar, and Bess B. Ward. 2011. “Ammonia Oxidation Rates and Nitrification in the Arabian Sea.” *Global Biogeochemical Cycles* 25 (4): 1–10. https://doi.org/10.1029/2010GB003940.

Newell, Silvia E., Sarah E. Fawcett, and Bess B. Ward. 2013. “Depth Distribution of Ammonia Oxidation Rates and Ammonia-Oxidizer Community Composition in the Sargasso Sea.” *Limnology and Oceanography* 58 (4): 1491–1500. https://doi.org/10.4319/lo.2013.58.4.1491.

Nowka, Boris, Holger Daims, and Eva Spieck. 2015. “Comparison of Oxidation Kinetics of Nitrite-Oxidizing Bacteria : Nitrite Availability as a Key Factor in Niche Differentiation” 81 (2): 745–53. https://doi.org/10.1128/AEM.02734-14.

Olsen, Are, Alex Kozyr, Siv K. Lauvset, Mario Hoppema, Fiz F. Pérez, Reiner Steinfeldt, Sara Jutterström, et al. 2016. “The Global Ocean Data Analysis Project Version 2 (GLODAPv2) – an Internally Consistent Data Product for the World Ocean.” *Earth System Science Data* 8 (2): 297–323. https://doi.org/10.5194/essd-8-297-2016.

Olson, RJ. 1981a. “15N Tracer Studies of the Primary Nitrite Maximum.” *Journal of Marine Research* 39 (Number 2): 203–26.

———. 1981b. “Differential Photoinhibition of Marine Nitrifying Bacteria - a Possible Mechanism for the Formation of the Primary Nitrite Maximum.” *Journal of Marine Research* 39 (2): 227–38.

Orsi, H, Thomas Whitworth, and Worth D Nowlin Jr. 1995. “On the Meridional Extent and Fronts of the Antarctic Circumpolar Current Pronounced Meridional Gradients in Surface Properties Separate Waters of the Southern Ocean from the Warmer and Saltier Waters of the Subtropical Circulations . Deacon (1933 , the S.” *Deep Sea Research* 42 (5): 641–73. https://doi.org/10.1016/0967-0637(95)00021-W.

Pachiadaki, Maria G, Eva Sintes, Kristin Bergauer, Julia M Brown, Nicholas R Record, Brandon K Swan, and Mary Elizabeth Mathyer. 2017. “Major Role of Nitrite-Oxidizing Bacteria in Dark Ocean Carbon Fixation” 1051 (November): 1046–51.

Peng, Xuefeng, Sarah E. Fawcett, Nicolas van Oostende, Martin J. Wolf, Dario Marconi, Daniel M. Sigman, and Bess B. Ward. 2018. “Nitrogen Uptake and Nitrification in the Subarctic North Atlantic Ocean.” *Limnology and Oceanography*, no. 1967. https://doi.org/10.1002/lno.10784.

Peng, Xuefeng, Clara A. Fuchsman, Amal Jayakumar, Sergey Oleynik, Willm Martens-Habbena, Allan H. Devol, and Bess B. Ward. 2015. “Ammonia and Nitrite Oxidation in the Eastern Tropical North Pacific.” *Global Biogeochemical Cycles* 29 (12): 2034–49. https://doi.org/10.1002/2015GB005278.

Peng, Xuefeng, Clara A. Fuchsman, Amal Jayakumar, Mark J. Warner, Allan H. Devol, and Bess B. Ward. 2016. “Revisiting Nitrification in the Eastern Tropical South Pacific: A Focus on

1139 Controls." *Journal of Geophysical Research: Oceans*. https://doi.org/10.1002/2015JC011455.

1140 Philibert, R., H. Waldron, and D. Clark. 2015. "A Geographical and Seasonal Comparison of
1141 Nitrogen Uptake by Phytoplankton in the Southern Ocean." *Ocean Science* 11 (2): 251–67.
1142 https://doi.org/10.5194/os-11-251-2015.

1143 Pollard, R. T., M. I. Lucas, and J. F. Read. 2002. "Physical Controls on Biogeochemical Zonation in
1144 the Southern Ocean." *Deep-Sea Research Part II: Topical Studies in Oceanography* 49 (16):
1145 3289–3305. https://doi.org/10.1016/S0967-0645(02)00084-X.

1146 Qin, Wei, Shady A. Amin, Rachel A. Lundeen, Katherine R. Heal, Willm Martens-Habbena, Serdar
1147 Turkarslan, Hidetoshi Urakawa, et al. 2018. "Stress Response of a Marine Ammonia-Oxidizing
1148 Archaeon Informs Physiological Status of Environmental Populations." *ISME Journal* 12 (2):
1149 508–19. https://doi.org/10.1038/ismej.2017.186.

1150 Qin, Wei, Shady A. Amin, Willm Martens-Habbena, Christopher B. Walker, Hidetoshi Urakawa,
1151 Allan H. Devol, Anitra E. Ingalls, James W. Moffett, E. Virginia Armbrust, and David A. Stahl.
1152 2014. "Marine Ammonia-Oxidizing Archaeal Isolates Display Obligate Mixotrophy and Wide
1153 Ecotypic Variation." *Proceedings of the National Academy of Sciences of the United States of*
1154 *America* 111 (34): 12504–9. https://doi.org/10.1073/pnas.1324115111.

1155 Raes, Eric J., Jodie van de Kamp, Levente Bodrossy, Allison A. Fong, Jessica Riekenberg, Bronwyn
1156 H. Holmes, Dirk V. Erler, Bradley D. Eyre, Sarah Sophie Weil, and A. M. Waite. 2020. "N2
1157 Fixation and New Insights Into Nitrification From the Ice-Edge to the Equator in the South
1158 Pacific Ocean." *Frontiers in Marine Science* 7 (May): 1–20.
1159 https://doi.org/10.3389/fmars.2020.00389.

1160 Raven, J. A., and P. G. Falkowski. 1999. "Oceanic Sinks for Atmospheric CO2." *Plant, Cell and*
1161 *Environment* 22 (6): 741–55. https://doi.org/10.1046/j.1365-3040.1999.00419.x.

1162 Read, J. F., R. T. Pollard, and U. Bathmann. 2002. "Physical and Biological Patchiness of an Upper
1163 Ocean Transect from South Africa to the Ice Edge near the Greenwich Meridian." *Deep-Sea*
1164 *Research Part II: Topical Studies in Oceanography* 49 (18): 3713–33.
1165 https://doi.org/10.1016/S0967-0645(02)00108-X.

1166 Rees, Andrew P., Ian Joint, and Kirsten M. Donald. 1999. "Early Spring Bloom Phytoplankton-
1167 Nutrient Dynamics at the Celtic Sea Shelf Edge." *Deep-Sea Research Part I: Oceanographic*
1168 *Research Papers*. https://doi.org/10.1016/S0967-0637(98)00073-9.

1169 Saito, Mak A., Matthew R. McIlvin, Dawn M. Moran, Alyson E. Santoro, Chris L. Dupont, Patrick A.
1170 Rafter, Jaclyn K. Saunders, et al. 2020. "Abundant Nitrite-Oxidizing Metalloenzymes in the
1171 Mesopelagic Zone of the Tropical Pacific Ocean." *Nature Geoscience* 13 (5): 355–62.
1172 https://doi.org/10.1038/s41561-020-0565-6.

1173 Santoro, A. E., C. M. Sakamoto, J. M. Smith, J. N. Plant, A. L. Gehman, A. Z. Worden, K. S.
1174 Johnson, C. A. Francis, and K. L. Casciotti. 2013. "Measurements of Nitrite Production in and
1175 around the Primary Nitrite Maximum in the Central California Current." *Biogeosciences* 10
1176 (11): 7395–7410. https://doi.org/10.5194/bg-10-7395-2013.

1177 Santoro, Alyson E., Christopher L. Dupont, R. Alex Richter, Matthew T. Craig, Paul Carini, Matthew
1178 R. McIlvin, Youngik Yang, William D. Orsi, Dawn M. Moran, and Mak A. Saito. 2015.
1179 "Genomic and Proteomic Characterization of 'Candidatus Nitrosopelagicus Brevis': An
1180 Ammonia-Oxidizing Archaeon from the Open Ocean." *Proceedings of the National Academy of*
1181 *Sciences of the United States of America* 112 (4): 1173–78.
1182 https://doi.org/10.1073/pnas.1416223112.

1183 Schaefer, Sylvia C., and James T. Hollibaugh. 2017. "Temperature Decouples Ammonium and Nitrite
1184 Oxidation in Coastal Waters." *Environmental Science and Technology* 51 (6): 3157–64.
1185 https://doi.org/10.1021/acs.est.6b03483.

https://doi.org/10.5194/bg-2021-280
Preprint. Discussion started: 29 October 2021

1186 Schofield, Oscar, Travis Miles, Anne Carlijn Alderkamp, Sang Hoon Lee, Christina Haskins, Emily
1187 Rogalsky, Rachel Sipler, Robert M. Sherrell, and Patricia L. Yager. 2015. “In Situ
1188 Phytoplankton Distributions in the Amundsen Sea Polynya Measured by Autonomous Gliders.”
1189 *Elementa*. https://doi.org/10.12952/journal.elementa.000073.

1190 Schramm, Andreas, Dirk DeBeer, Johan van den Heuvel, Simon Ottengraf, and Rudolf Amann. 1999.
1191 “Microscale Distribution of Populations and Activities of Nitrosospira and Nitrospira Spp. along
1192 a Macroscale Gradient in a Nitrifying Bioreactor: Quantification by In Situ Hybridization and
1193 the Use of Microsensors.” *Society* 65 (8): 3690–96.

1194 Sciandra, A., and R. Amara. 1994. “Effects of Nitrogen Limitation on Growth and Nitrite Excretion
1195 Rates of the Dinoflagellate Prorocentrum Minimum.” *Marine Ecology Progress Series* 105 (3):
1196 301. https://doi.org/10.3354/meps105301.

1197 Shafiee, Roxana T., Joseph T. Snow, Qiong Zhang, and Rosalind E. M. Rickaby. 2019. “Iron
1198 Requirements and Uptake Strategies of the Globally Abundant Marine Ammonia-Oxidising
1199 Archaeon, Nitrosopumilus Maritimus SCM1.” *The ISME Journal*.
1200 https://doi.org/10.1038/s41396-019-0434-8.

1201 Sigman, D. M., K. L. Casciotti, M. Andreani, C. Barford, M. Galanter, and J. K. Böhlke. 2001. “A
1202 Bacterial Method for the Nitrogen Isotopic Analysis of Nitrate in Seawater and Freshwater.”
1203 *Analytical Chemistry* 73 (17): 4145–53. https://doi.org/10.1021/ac010088e.

1204 Smart, Sandi M, Sarah E Fawcett, Sandy J Thomalla, Mira a Weigand, Chris J C Reason, and Daniel
1205 M Sigman. 2015. “Global Biogeochemical Cycles,” 1–19.
1206 https://doi.org/10.1002/2014GB005013.Received.

1207 Sorokin, Dimitry Y., Sebastian Lücker, Dana Vejmelkova, Nadezhda A. Kostrikina, Robbert
1208 Kleerebezem, W. Irene C. Rijpstra, Jaap S. Sinninghe Damsté, et al. 2012. “Nitrification
1209 Expanded: Discovery, Physiology and Genomics of a Nitrite-Oxidizing Bacterium from the
1210 Phylum Chloroflexi.” *ISME Journal* 6 (12): 2245–56. https://doi.org/10.1038/ismej.2012.70.

1211 Spieck, Eva, Silke Ehrich, and Jens Aamand. 1998. “Isolation and Immunocytochemical Location of
1212 the Nitrite-Oxidizing System in Nitrospira Moscoviensis.” *Arch Microbiol*, no. 169: 225–30.

1213 Spieck, Eva, S Muller, A Engel, E Mandelkow, H Patel, and E Bock. 1996. “Two-Dimensional
1214 Structure of Membrane-Bound Nitrite Oxidoreductase from Nitrobacter Hamburgensis.” *Journal
1215 of Structural Biology* 117 (0076): 117–23.

1216 Starkenburg, Shawn R., Patrick S.G. Chain, Luis A. Sayavedra-Soto, Loren Hauser, Miriam L. Land,
1217 Frank W. Larimer, Stephanie A. Malfatti, et al. 2006. “Genome Sequence of the
1218 Chemolithoautotrophic Nitrite-Oxidizing Bacterium Nitrobacter Winogradskyi Nb-255.”
1219 *Applied and Environmental Microbiology*. https://doi.org/10.1128/AEM.72.3.2050-2063.2006.

1220 Sun, Xin, Claudia Frey, Emilio Garcia-Robledo, Amal Jayakumar, and Bess B. Ward. 2021.
1221 “Microbial Niche Differentiation Explains Nitrite Oxidation in Marine Oxygen Minimum
1222 Zones.” *The ISME Journal*, 1–13. https://doi.org/10.1038/s41396-020-00852-3.

1223 Sun, Xin, Qixing Ji, Amal Jayakumar, and Bess B. Ward. 2017. “Dependence of Nitrite Oxidation on
1224 Nitrite and Oxygen in Low-Oxygen Seawater.” *Geophysical Research Letters* 44 (15): 7883–91.
1225 https://doi.org/10.1002/2017GL074355.

1226 Sundermeyer-Klinger, Hilke, Wolfgang Meyer, Beate Warninghoff, and Eberhard Bock. 1984.
1227 “Membrane-Bound Nitrite Oxidoreductase of Nitrobacter: Evidence for a Nitrate Reductase
1228 System.” *Archives of Microbiology* 140 (2–3). https://doi.org/10.1007/BF00454918.

1229 Tagliabue, A., T. Mtshali, O. Aumont, A. R. Bowie, M. B. Klunder, A. N. Roychoudhury, and S.
1230 Swart. 2012. “A Global Compilation of Dissolved Iron Measurements: Focus on Distributions
1231 and Processes in the Southern Ocean.” *Biogeosciences* 9 (6): 2333–49.

https://doi.org/10.5194/bg-9-2333-2012.

Tsoularis, A, and J Wallace. 2002. "Analysis of Logistic Growth Models." *Mathematical Biosciences* 179: 21–55.

Ushiki, Norisuke, Masaru Jinno, Hirotsugu Fujitani, Toshikazu Suenaga, Akihiko Terada, and Satoshi Tsuneda. 2017. "Nitrite Oxidation Kinetics of Two Nitrospira Strains : The Quest for Competition and Ecological Niche Differentiation." *Journal of Bioscience and Bioengineering* 123 (5): 581–89. https://doi.org/10.1016/j.jbiosc.2016.12.016.

Vaccaro, Ralph F, and John H Ryther. 1960. "Marine Phytoplankton and the Distribution of Nitrite in the Sea*." *ICES Journal of Marine Science* 25 (3): 260–71. https://doi.org/10.1093/icesjms/25.3.260.

Vajrala, Neeraja, Willm Martens-Habbena, Luis A. Sayavedra-Soto, Andrew Schauer, Peter J. Bottomley, David A. Stahl, and Daniel J. Arp. 2013. "Hydroxylamine as an Intermediate in Ammonia Oxidation by Globally Abundant Marine Archaea." *Proceedings of the National Academy of Sciences of the United States of America* 110 (3): 1006–11. https://doi.org/10.1073/pnas.1214272110.

Volk, T., and M. I. Hoffert. 1985. "Ocean Carbon Pumps: Analysis of Relative Strengths and Efficiencies in Ocean-Driven Atmospheric CO2 Changes." *The Carbon Cycle and Atmospheric CO*.

Walker, C. B., J. R. De La Torre, M. G. Klotz, H. Urakawa, N. Pinel, D. J. Arp, C. Brochier-Armanet, et al. 2010. "Nitrosopumilus Maritimus Genome Reveals Unique Mechanisms for Nitrification and Autotrophy in Globally Distributed Marine Crenarchaea." *Proceedings of the National Academy of Sciences of the United States of America* 107 (19): 8818–23. https://doi.org/10.1073/pnas.0913533107.

Ward, B. B. 2005. "Temporal Variability in Nitrification Rates and Related Biogeochemical Factors in Monterey Bay, California, USA." *Marine Ecology Progress Series* 292: 97–109. https://doi.org/10.3354/meps292097.

———. 2008. "Chapter 5 - Nitrification in Marine Systems." In *Nitrogen in the Marine Environment (2nd Edition)*, 199–261. https://doi.org/http://dx.doi.org/10.1016/B978-0-12-372522-6.00005-0.

Ward, B. B., and K. A. Kilpatrick. 1991. "Nitrogen Transformations in the Oxic Layer of Permanent Anoxic Basins: The Black Sea and the Cariaco Trench." In *Black Sea Oceanography*. https://doi.org/10.1007/978-94-011-2608-3_7.

Ward, B. B., and O. C. Zafiriou. 1988. "Nitrification and Nitric Oxide in the Oxygen Minimum of the Eastern Tropical North Pacific." *Deep Sea Research Part A, Oceanographic Research Papers* 35 (7): 1127–42. https://doi.org/10.1016/0198-0149(88)90005-2.

Watson, Andrew J., Ute Schuster, Jamie D. Shutler, Thomas Holding, Ian G.C. Ashton, Peter Landschützer, David K. Woolf, and Lonneke Goddijn-Murphy. 2020. "Revised Estimates of Ocean-Atmosphere CO2 Flux Are Consistent with Ocean Carbon Inventory." *Nature Communications* 11 (1): 1–6. https://doi.org/10.1038/s41467-020-18203-3.

Watson, Stanley W., Eberhard Bock, Frederica W. Valois, John B. Waterbury, and Ursula Schlosser. 1986. "Nitrospira Marina Gen. Nov. Sp. Nov.: A Chemolithotrophic Nitrite-Oxidizing Bacterium." *Archives of Microbiology*. https://doi.org/10.1007/BF00454947.

Watson, Stanley W., and John B. Waterbury. 1971. "Characteristics of Two Marine Nitrite Oxidizing Bacteria,." *Microscopy* 77 (2631): 203–30.

Xu, Min Nina, Xiaolin Li, Dalin Shi, Yao Zhang, Minhan Dai, Tao Huang, Patricia M. Glibert, and Shuh Ji Kao. 2019. "Coupled Effect of Substrate and Light on Assimilation and Oxidation of Regenerated Nitrogen in the Euphotic Ocean." *Limnology and Oceanography* 64 (3): 1270–83.

https://doi.org/10.5194/bg-2021-280
Preprint. Discussion started: 29 October 2021

https://doi.org/10.1002/lno.11114.

Yool, Andrew, Adrian P Martin, Camila Fernández, and Darren R Clark. 2007. "The Significance of Nitrification for Oceanic New Production." *Nature* 447 (7147): 999–1002. https://doi.org/10.1038/nature05885.

Zakem, Emily J., Alia Al-Haj, Matthew J. Church, Gert L. Van Dijken, Stephanie Dutkiewicz, Sarah Q. Foster, Robinson W. Fulweiler, Matthew M. Mills, and Michael J. Follows. 2018. "Ecological Control of Nitrite in the Upper Ocean." *Nature Communications* 9 (1). https://doi.org/10.1038/s41467-018-03553-w.

Zhang, Yao, Wei Qin, Lei Hou, Emily J. Zakem, Xianhui Wan, Zihao Zhao, Li Liu, et al. 2020. "Nitrifier Adaptation to Low Energy Flux Controls Inventory of Reduced Nitrogen in the Dark Ocean." *Proceedings of the National Academy of Sciences of the United States of America* 117 (9): 4823–30. https://doi.org/10.1073/pnas.1912367117.